Annelise E. Barron
Harvey W. Blanch
David S. Soane

Department of Chemical Engineering, University of California, Berkeley, CA

A transient entanglement coupling mechanism for DNA separation by capillary electrophoresis in ultradilute polymer solutions

Using capillary electrophoresis, large DNA molecules (2.0–23.1 kbp) may be rapidly separated in ultradilute polymer solutions (< 0.002% w/w) under a high-voltage, steady field (265 V/cm). At this polymer concentration, the separation mechanism appears to be significantly different from that postulated to occur in crosslinked gels. Based on experimental results obtained with DNA restriction fragments and with negatively charged latex microspheres, we conclude that the Ogston and reptation models typically used to describe gel electrophoresis are not appropriate for DNA separations in such dilute polymer solutions. Electrophoresis experiments employing solutions of both small and large hydroxyethyl cellulose polymers highlight the importance of polymer length and concentration for the optimum resolution of DNA fragments varying in size from 72 bp to 23.1 kbp. A transient entanglement coupling mechanism for DNA separation in dilute polymer solutions is developed, which suggests that there is no *a priori* upper size limit to DNA that can be separated by capillary electrophoresis in a constant field.

1 Introduction

Restriction mapping of chromosomal DNA may require the electrophoretic separation of restriction fragments ranging in size from a few hundred to several million base pairs, depending on the organism under study and the stage of the mapping effort [1]. DNA electrophoresis is generally conducted in gels because the free-solution electrophoretic mobility of DNA, a homologous macroanion, is independent of molecular size [2, 3]. For sequencing and fine mapping, DNA fragments smaller than ~ 2 kbp can be separated with high resolution by steady-field electrophoresis in crosslinked polyacrylamide slab gels, generally in less than 45 min. DNA fragments ranging from 2–40 kbp are typically separated in larger pore-size agarose slab gels under a low, steady electric field, requiring up to 2 h. On the other hand, the electrophoretic separation of DNA restriction fragments larger than 40 kbp is currently one of the slowest steps in the process of mapping and sequencing the human genome. These separations can only be achieved using low-voltage pulsed fields, and typically require more than 20 h of electrophoresis in agarose slab gels [4–6]. For both pulsed-field and steady-field slab gel electrophoresis, detection of DNA bands typically involves either (i) initial hybridization of the DNA mixture of interest with radioactive [^{32}P]ATP labeled probes, followed by electrophoretic separation and autoradiography [7], or (ii) postelectrophoretic gel staining with carcinogenic intercalating dyes such as ethidium bromide, followed by fluorescence imaging. This process is labor-intensive, time-consuming, potentially hazardous, and involves several manual steps that are not amenable to automation.

Correspondence: Professor David S. Soane, Department of Chemical Engineering, 201 Gilman Hall, University of California, Berkeley, CA 94720, USA

Abbreviations: Ferguson plot, plot of log(absolute mobility) *vs.* gel or sieving polymer concentration; **HEC,** hydroxyethyl cellulose; **TBE,** Tris-boric acid-EDTA

Capillary electrophoresis (CE), a separation technique that employs a fused-silica capillary (ID 25–100 μm) and on-line UV absorbance or fluorescence detection, has been shown to be not only up to 25 times faster, but potentially much more reproducible and efficient for DNA separations than slab gel electrophoresis (see, for example [8–18]). Yet, ten years after its introduction [19], the technique of CE is still not widely used by molecular biologists for DNA electrophoresis. This is because several practical aspects of the technique must be improved before the efficiency and speed of CE will outweigh the familiarity and versatility of slab gels. For example, in slab gels many lanes are generally run in parallel, an important step in techniques such as DNA sequencing and DNase footprinting [7]. Strategies for multiplexing capillaries so that several "lanes" can be run in parallel are still under development [20], as are methods for post-electrophoretic sample collection [10, 13, 21–24]. One of the most active areas of research in capillary electrophoresis, however, is the search for inter-capillary DNA sieving matrices that give highly reproducible electrophoretic mobilities and long-term stability under high electric fields, and which are easy and cost-effective to use.

The geometry of a microbore, fused-silica capillary offers both advantages and drawbacks for DNA electrophoresis, as opposed to separation by slab gel electrophoresis. One major advantage is the high surface area-to-volume ratio, which provides rapid dissipation of Joule heat and allows electric fields up to 400 V/cm to be used without a substantial temperature increase [14]. However, the capillary geometry places different demands on the DNA separation matrix than those required in a slab format. Gel polymerization inside a capillary, without the formation of shrinkage-induced bubbles and other inhomogeneities, is difficult. Bubbles can also be formed in the gel during electrophoresis, leading to a variation in DNA electrophoretic mobility. The preparation of gel-filled capillaries of uniform quality and stability, such as would be preferred for a multiple-capillary array, has been fraught with such difficulties and is still a matter of discussion in the literature [25–30].

© VCH Verlagsgesellschaft mbH, 69451 Weinheim, 1994

0173-0835/94/0505-0597 $5.00+.25/0

To date, research on the preparation of gel-filled capillaries for DNA separation has focused almost exclusively on the use of polyacrylamide gels. Although polyacrylamide gel-filled capillaries have demonstrated great potential for the single-base pair resolution of DNA up to 450 bp (necessary for DNA sequencing) [22, 25, 26, 29, 31–34], their applicability for DNA restriction mapping is limited. The structure of crosslinked polyacrylamide is such that it can only separate DNA smaller than ~ 2 kbp, making it inadequate for most mapping separations. Agarose gels, although useful as slabs for restriction mapping of large DNA, appear to be a less effective medium for capillary electrophoresis than polyacrylamide. Within a capillary, agarose gels apparently yield relatively poor separations [35, 36], and furthermore do not form an optically transparent separation matrix, complicating the detection of analytes. Therefore, no known crosslinked gel matrix is effective for the CE separations of DNA restriction fragments longer than 2 kbp.

In a traditional slab geometry, the gel fulfills two roles: (i) its high density and rigidity prevent the convection and diffusion of analytes that would cause band broadening, and (ii) it provides size-based separation of homologous macroions such as DNA and SDS-proteins that cannot be separated in free solution. One of the most striking advantages of using capillary electrophoresis for DNA separations is that in a capillary (ID < 100 μm), convection and diffusion have a negligible effect on band-broadening even at high fields [14], and thus rigidity of the internal separation matrix is not required. Consequently, crosslinking or gelation of the polymers is unnecessary, and the problems of inter-capillary gel polymerization can be avoided. The use of an uncrosslinked separation matrix for the electrophoresis of macroions was pioneered by Bode on strips of cellulose acetate coated with agar or polyacrylamide [37], and later applied to capillary electrophoresis by Zhu *et al.* [11] and Chin *et al.* [38]. Since then, solutions of many different uncrosslinked polymers have been employed as separation media for capillary electrophoresis of DNA, including glucomannan [39], polyethylene glycol and dextran [40, 41], linear polyacrylamide [12, 15, 42–44], and hydrophilic cellulose derivatives [42, 45–50].

Uncrosslinked polymer solutions are able to separate DNA much larger than 2 kbp, as well as restriction fragments smaller than 100 bp, depending on the specific polymer and its concentration. Strege and Lagu separated λ-*Hin*dIII restriction fragments 2 kbp–23.1 kbp in size with fairly good resolution using 0.50% methylcellulose [46]. Chiari *et al.* [44] have achieved excellent separations of DNA as large as 23.1 kbp in extremely viscous, 4.5% polyacrylamide, after performing *in situ* polymerization of the acrylamide and 1 h of preelectrophoresis to remove charged catalysts remaining after the polymerization reaction. Restriction fragments as large as 12 kbp have been separated with 10-base pair resolution in melted agarose solutions having concentrations greater than 1.0% [16], as well as in 0.40% methylcellulose [51], and sparsely crosslinked polyacrylamide (3%T, 0.5% C) [12]. In all three of these polymer media, however, baseline resolution began to degrade for DNA larger than 5 kbp, and was quite poor for fragments larger than 10 kbp. It is unlikely that these results represent the upper size limit of this CE technique, however. None of these studies tested the effect of polymer chain length on resolution. In our studies with hydroxyethyl cellulose (HEC) solutions, we have not only shown that chain length is important in resolving power, but also that resolution of large DNA fragments (> 1 kbp) is generally best achieved at *low* concentrations of relatively long polymers [48]. Chrambach *et al.* reached the same conclusion using high-molecular weight linear polyacrylamide to separate DNA as large as 48.5 kbp [15]. We will discuss the possible reasons for this phenomenon later.

While DNA sequencing requires single-base pair resolution, for DNA restriction mapping, resolution of fragments differing by 10 base pairs is generally considered sufficient. While 10-base pair resolution has been reported using 4–6%T linear polyacrylamide [12, 44, 52], 0.22% HEC [48], and 0.5% methylcellulose [46], single-base pair resolution has been achieved in uncrosslinked polymer solutions upon the addition of ethidium bromide to the running buffer [53], presumably because the intercalator lengthens and stiffens the DNA [54], changing its physical properties in an advantageous manner.

To date, it remains unclear which is the best polymer, and what is the optimum concentration range, to use for DNA separations by CE. This is because few systematic studies, such as those undertaken by Chrambach's group [17, 55, 56] and Righetti's group [44] exist in the literature; the bulk of experimental evidence is primarily anecdotal. Uncrosslinked polymer solutions have been shown to separate DNA over a wide range of concentrations, from semidilute, low-viscosity solutions of cellulosic polymers (0.10–1.00%) [46–49, 51] to extremely concentrated, "syrupy" polyacrylamide solutions (≥ 10% T, 0% C), so viscous that they cannot be injected into a capillary and must be polymerized *in situ* [18, 44]. The primary advantage of using low-viscosity polymer solutions is that they form a replaceable sieving matrix, allowing easy filling, flushing, and refilling of the capillary between uses. Thus, one capillary may be used for several weeks. This is desirable because manual replacement and alignment of the fine, hair-like capillaries is a difficult process requiring both patience and dexterity. Like gel-filled capillaries, capillaries filled with extremely concentrated polymer solutions must be discarded after the useful lifetime of one separation matrix, generally no more than 30 runs [18, 44].

Certain questions, such as why the presence of ethidium bromide improves DNA resolution in uncrosslinked polymer solutions [53], and why linear polyacrylamide must be used at higher concentrations than cellulose derivatives to give comparable separations, cannot be answered until more is known about the mechanism of DNA separation in uncrosslinked polymer solutions. Some researchers have asserted that the mechanism is essentially the same as that in traditional slab gel electrophoresis, *i.e.*, that transient "pores" are formed in the polymer solutions [17, 36, 42, 45, 47, 57], while others have attributed separation to the attraction and interac-

tion of DNA fragments with the polymers in the buffer, without specifying these interactions [38, 46].

Grossman and Soane [47] proposed that, for polymers in dilute solution to be effective for DNA separation, they must be entangled; and that it was the physical similarity of this entangled network to the "pore network" of a gel which allowed size-dependent separation of DNA. A polymer solution is entangled if it is well above the overlap threshold concentration (Φ^*), *i.e.*, the concentration at which the polymer chains begin to interact strongly in solution [58]. This concentration can be estimated from a plot of solution viscosity *vs.* polymer concentration. In dilute solution, when there is no strong interaction between polymer molecules, viscosity increases in direct proportion to polymer concentration, and the slope of this plot is constant at about 1.0. The formation of an incipient entangled polymer network in solution [59] is evidenced by a large increase in viscosity, with a corresponding increase in the slope of the viscosity *vs.* concentration curve. Furthermore, the overlap threshold concentration of HEC was shown to be strongly dependent on the length of the HEC chain [48]. This dependence is well described by the equation

$$\Phi^* = 3.63\left[\frac{M_n}{M_0}\right]^{-1.2} + 1.18 \times 10^{-4} \quad (1)$$

where M_n is the number-average HEC molecular weight and M_0 is the average monomer molecular weight (272 g/mol for HEC with a molar substitution of 2.5) [48]. We have shown in a recent paper [48] that DNA separation is possible in dilute (*i.e.*, nonentangled) HEC solutions with concentrations well below the measured Φ^*. This confirms the recent theoretical prediction of Viovy and Duke that duplex DNA up to 1 kbp or more could be separated in dilute, nonentangled solutions of high molecular weight polymers [60].

Viovy and Duke [60] have also suggested, however, that using the point of departure from linearity of the viscosity *vs.* concentration curve is an ambiguous criterion for the determination of Φ^*, since it depends upon the accuracy with which the experimenter can evaluate the linearity of the data. Instead, they suggest using an equation derived from polymer physics [61] Φ^*:

$$\Phi^* \cong 3\ M_w/4\ \pi N_A R_p^3 \cong 0.6\ [\eta]^{-1} \quad (2)$$

where M_w is the weight-average molecular weight of the polymer, N_A is Avogadro's number, R_p is the polymer's radius of gyration in solution, and $[\eta]$ is the intrinsic viscosity of the polymer in the solvent of interest. The first half of Eq. (2) is a purely geometrical definition of the overlap theshold, equating Φ^* to the concentration at which the polymers, modeled as spherical coils, statistically touch in solution. Reliable determination of Φ^* by this equation requires accurate knowledge of R_p in various solvent conditions, as well as knowledge of the weight-average molecular weight. The second half of Eq. (2) relies simply on knowledge of the intrinsic viscosity. This is a sensible approach, as it potentially could save researchers the time and effort involved in taking viscosity *vs.* concentration data to determine Φ^*, if the intrinsic viscosity of the polymer sample in the solvent of interest was already known. However, it is not difficult or ambiguous to determine the point of departure from linearity of the viscosity *vs.* concentration data; the viscosity increase upon entanglement is pronounced (see for example [48]).

The question of interest is whether DNA is separated by the same mechanism in both uncrosslinked polymer solutions and in gels. If so, the same models that are commonly used for gel electrophoresis would be applicable to non-gel separations. The structures of polyacrylamide and agarose gels are generally modeled as topologically static "pore networks" [62], and it is thought that DNA separation arises because movement through these "pores" alters DNA frictional properties in a size-dependent manner. Yet the actual mechanism of the molecular weight separation of double-stranded DNA fragments in gels is still not completely understood [63, 64]. Although present models are successful in fitting experimental data in certain regimes of DNA size and electric field strength, no single model can fully explain the dependence of electrophoretic mobility on molecular weight, gel concentration, temperature, and electric field strength.

Two theories are commonly used to model DNA electrophoresis in gels: the Ogston model, and the reptation model. In the original Ogston theory, proposed in 1958 [65], the gel is modeled as a static, infinite network of long, inert and randomly distributed linear fibers, with a negligible number of chain ends. This random fiber network is characterized with a certain "average pore size". A polymeric macro-ion such as DNA is assumed to electrophorese through this network as an unperturbed spherical coil, which must diffuse laterally until it encounters a pore large enough in diameter to permit its passage [66–68]. The mobility is dependent upon the volume fraction of the gel which is available to the undeformed spherical coil. According to this purely geometrical model, DNA coils much larger in radius than the gel pores would not be able to enter the gel at all. Until recently, the Ogston model was considered to be useful only for fitting experimental data for small DNA fragments (with radii of gyration comparable to or smaller than the average pore size) in the limit of low electric fields [69, 70]. The applicability of the Ogston model has been typically ascertained by use of a semilogarithmic plot of DNA electrophoretic mobility *vs.* gel concentration (a Ferguson plot). Accordingly, a Ferguson plot should be linear, with a slope of $K_r = k(r + R_g)^2$, where K_r is the "retardation coefficient", k is a constant of proportionality, r is the radius of the gel fiber, and R_g is the radius of gyration of the DNA molecule [66–68]. When Ferguson plots were found to be nonlinear (usually concave) for gel electrophoresis of DNA molecules larger than a few hundred base pairs [71], it was reasoned that the slope of the Ferguson plot was changing with increasing gel concentration because the equivalent radius of the DNA, as well as the gel fiber radius, were functions of the gel concentration [72]. It was hypothesized, specifically for agarose gels, that as gel concentration increases, the radius of the supercoiled agarose gel fiber decreases and the total fiber length increases to

approach the dimension of the single-stranded agarose double helix [72]. An "extended Ogston model" was developed by Tietz and Chrambach *et al.* (*e.g.*, [72–74], in which the retardation coefficient was allowed to depend on the gel concentration, as well as the DNA radius of gyration and gel fiber radius. In this revised Ogston model, nonlinear curve-fitting was applied to concave or convex Ferguson plots to determine "local retardation coefficients" for large DNA molecules (up to thousands of base pairs long) (*e.g.*, [15–17]). Except for a provision allowing the gel fiber radius to change with gel concentration, the basic geometrical assumptions of the model concerning the separation matrix remain the same as in the original Ogston model, however, and intrinsic properties of the gel fibers (such as flexibility) are not considered.

The geometrical assumptions of the original Ogston model are invalid for larger DNA, since DNA with radii of gyration much larger than the estimated average pore radius can still migrate through the gel during electrophoresis. It is clear, then, that DNA molecules must stretch and change shape under certain conditions to move through constrictive spaces in the gel. Experimentally, DNA smaller than ~ 40 kbp undergoes steady-field size separation in agarose gels. Larger DNA migrates as a single band, even at low fields, and can only be separated by pulsed-field electrophoresis [4, 5]. The reptation model was developed to explain these findings [69, 75, 76]. This model is based on the assumption that randomly coiled DNA molecules too large to fit through a pore while maintaining a coiled conformation will migrate head-first, snake-like, through "tubes" formed by the pore network of the gel; no lateral motion is allowed within the tube. DNA molecules are thought to alternately stretch and relax as they slither through the tubes, due to their viscoelastic character [77]. The reptation model is able to provide a theoretical explanation for the experimentally observed regime in which electrophoretic mobility is inversely related to DNA size [69, 78].

The reptation model assumes that at high fields, and/or for DNA larger than ~ 40 kbp, field-induced orientation extends the stretching periods of the DNA, causing their random walk to become strongly biased in the forward direction (the biased reptation regime [79]), so that DNA is stretched to a rod-like conformation. Consequently, the electrophoretic mobility increases to a maximum, or "saturated" level [76], and size-based separation in a constant field diminishes dramatically. (It has been argued that such DNA stretching, as well as the inverse relation between DNA size and mobility, can also be explained using the extended Ogston model [73].) Typically, the logarithm of the mobility (extrapolated to zero field strength) is plotted as a function of the logarithm of inverse DNA size (in bp) to test for adherence to the reptation model. The curves generally have a sigmoidal shape, with a linear region in the center (*i.e.*, for intermediate DNA sizes) having a slope of −1.0. This linear region is attributed to the reptation (without DNA stretching) regime (see Fig. 3 of [69]). The nonlinear ends of the sigmoidal curve are thought to be the result of Ogston-type sieving (for small DNA) and biased reptation with DNA stretching (for large DNA) [69].

The Ogston model envisions DNA as a spherical random coil, moving through a random fiber network having a distribution of fractional volumes (pores) available for DNA passage and a negligible number of chain ends (*i.e.*, a static and infinite network of inert, noninteracting linear fibers). The reptation model, on the other hand, describes DNA conformation as extended and snake-like, and models the gel as a topologically static network of tube-like pores having a certain average radius. Bode [80, 81] has questioned both of these static concepts of a gel, particularly in the case of polyacrylamide, a vinyl polymer which would be expected to form a highly flexible and thus easily deformable gel network. Bode showed in 1979 that experimental results from polyacrylamide gel electrophoresis of macroions, which had been interpreted earlier as substantiation of the "rigid-pore" concept of a gel, could be equally well-explained by a viscosity model based on the assumption that gel molecules represent obstacles which must be cleared aside by the electrokinetic pressure of the migrating macroions [80].

In this paper, we show that the "rigid-pore" concept used to describe the mechanism of DNA separations in gels is not applicable to separations in dilute polymer solutions, and that a different theoretical framework, similar to that proposed by Bode [80], is necessary to understand DNA motion in this media. We investigate the dependence of DNA electrophoretic mobility on HEC concentration and molecular weight, giving particular attention to the minimum HEC concentration which is required to achieve DNA separation and the optimum HEC concentrations for separating DNA restriction fragments in particular size ranges. In addition, we examine the electrophoretic behavior of negatively charged polystyrene latex spheres in dilute HEC solutions, and compare these results to those achieved with double-stranded DNA having similar radii of gyration.

2 Materials and methods

2.1 Instrumentation

The CE apparatus used in these studies has been described elsewhere [47]. The apparatus employs a fused-silica capillary with an external coating of polyimide (Polymicro Technologies, Phoenix, AZ, USA) and no internal coating, 50 cm in length (35 cm to the detector), with ID 51 μm and OD 360 μm. The capillary connects the anodic reservoir with the electrically grounded cathodic reservoir. A high-voltage power supply with a 30 000 V capacity (Gamma High Voltage Research, Ormand Beach, CA, USA) was used to drive electrophoresis. Current was measured over a 1 kΩ resistor in the return circuit of the power supply, using a digital multimeter (Model 3465B, Hewlett-Packard, Palo Alto, CA, USA). On-column detection was by UV absorbance at 260 nm, using a modified variable-wavelength detector (Model 783, Applied Biosystems, Foster City, CA, USA). Data were collected using an integrator (Model 3390, Hewlett-Packard).

2.2 Materials

A ΦX174-*Hae*III rstriction digest was obtained from Bethesda Research Labs (Bethesda, MD, USA) at a concentration of 592 μg/mL. A nonstoichiometric mixture of λ-*Hin*dIII and ΦX174-*Hae*III restriction fragments (λ-*Hin*dIII fragments present at a lower concentration) was obtained from Pharmacia LKB Biotechnology (Alameda, CA, USA) at a concentration of 500 μg/mL. Monodisperse carboxylated polystyrene latex spheres (diameter 29.5 nm) were purchased from Polysciences (Warrington, PA, USA). Monidisperse sulfonated polystyrene lates spheres (diameters 61, 116, 132 nm) were a kind gift of Stephen Nilsen (Department of Chemical Engineering, Stanford University, Palo Alto, CA). Mesityl oxide was used as a neutral marker in all experiments to gauge electroosmotic velocity (Aldrich Chemical Co., Milwaukee, WI, USA). The buffer used in all experiments with DNA was 89 mM Tris, 89 mM boric acid, and 5 mM EDTA (TBE), with a pH of 8.15 (all buffer reagents purchased from Sigma, St. Louis, MO, USA). The buffer used in all experiments with charged colloidal spheres was 0.05 M sodium chloride, 0.05 M boric acid, 6 mM sodium hydroxide, pH 8.2 (buffer reagents purchased from Sigma), with 0.5% Triton X-100 nonionic surfactant (Polysciences), to prevent adsorption or aggregation of the microspheres. Surfactants were also found necessary in other electrophoresis studies using charged microspheres [82–86]. Measured amounts of HEC were added to buffer solutions; solutions were vigorously shaken, and then mixed for 24 h by tumbling (mechanical stirring sometimes led to incomplete dissolution). Successive dilution was used to make extremely dilute solutions. Two different HEC samples (obtained from Polysciences) were used, with molecular weights of $M_n \cong 24000–27000$ g/mol and $M_n \cong 90000–105000$ g/mol. Hereafter these samples will be referred to as HEC (M_n 27000) and HEC (M_n 105000). The molecular weights of these HEC samples were determined by the company.

2.3 CE

Before each experiment, the uncoated inner capillary wall was conditioned first with 1 M NaOH for 10 min, then with 0.1 M NaOH for 10 min, and finally with the electrophoresis buffer (containing dissolved HEC) for 15 min. The electric field was turned on and left on until current through the capillary had stabilized, usually 15–20 min. DNA samples containing λ-*Hin*dIII restriction fragments were pre-heated for 5 min at 65°C (restriction fragments of 4361 bp and 23130 bp have cohesive termini). All DNA samples were premixed with a minute amount of mesityl oxide, and injected without dilution. The four sphere samples were also premixed in buffer, and mesityl oxide was added to the sample, before injection. Samples were introduced to the anodic end of the capillary by applying a vacuum of 1–3 inchHg (13546 Pa) for a specific time which depended on the buffer viscosity, to introduce approximately 3 nL (3×10^{-6} cm^3) of sample for each run. After the sample slug was drawn into the capillary, the anodic end of the capillary was replaced in the electrophoresis buffer, together with the anodic electrode, and the electrophoretic voltage was applied. All experiments were run at a field strength of 13282 V (265 V/cm). The capillary was surrounded by an air bath at a temperature of 30.0 ± 0.1°C in all experiments.

We have employed the traditional approach used with uncoated capillaries, which is to hydrodynamically inject analyte at the anodic end and detect at the cathodic end [38]. Strong, constant electroosmotic flow moving in the cathodic direction pulls the negatively charged analytes (migrating by electrophoresis in the *anodic* direction) past the UV absorbance detector window. Thus, those analytes having the smallest electrophoretic mobility in the direction of the anode (*i.e.*, larger DNA or smaller spheres), pass the detector first as a result of electroosmotic flow, and will be followed by the faster ones, in order of increasing electrophoretic mobility. The peak order, then, is reversed from what is seen in the absence of electroosmotic flow. Absolute electrophoretic mobilities were calculated by subtracting the electroosmotic velocity per unit field strength (determined from the elution time of the neutral marker) from the apparent electrophoretic mobility of the negatively charged analyte, since they migrate in opposite directions; a mathematical description of this calculation can be found elsewhere [87]. For clarity, we note that the electroosmosis of the buffer is a bulk flow having a flat velocity profile [88], which exerts an equal force on all DNA molecules in the sample (*i.e.*, the electroosmotic velocity of the DNA is not molecular size-dependent) as well as on the neutral marker, mesityl oxide. This is demonstrated when electrophoresis is performed in the absence of polymers in the TBE buffer (*i.e.*, in free solution), DNA molecules elute from the capillary as a single peak.

When coated capillaries are used, as is more typical in the literature, the electroosmotic velocity of the buffer ist reduced to well below the electrophoretic velocity of the analytes; in this case, injection is usually performed electrokinetically at the cathodic end of the capillary and detection occurs at the anodic end. It is generally thought that superior resolution and reproducibility are obtained with coated capillaries, whose negative surface charge is neutralized by a covalently attached coating of hydrophilic polymers, thereby eliminating electroosmotic flow [46, 49, 89, 90]. However, since our primary interest was investigating the mechanism of DNA separation, rather than optimizing the technique, we found it less complicated to use uncoated capillaries. It is true that in early capillary electrophoresis experiments, electroosmotic flow in uncoated silica capillaries was associated with unreproducibility of analyte migration velocity [91]. Since separation of similar species is dependent upon small differences in electrophoretic mobility, it is important that the analytes' net migration times, which have both an electrophoretic and an electroosmotic velocity component, be highly reproducible. In uncoated capillaries, the run-to-run reproducibility of electroosmotic velocity in a given capillary is dramatically improved by prerun caustic rinses. Rinses of 4 to 6 capillary volumes with 1 M NaOH or KOH followed by a six-capillary volume rinse with the running buffer has been shown to give net migration times which are repro-

ducible to within 2% [92]. Using this method, we also obtained excellent reproducibility, generally finding run-to-run standard deviations in absolute DNA electrophoretic mobility of less than 0.50%. Technically, although the capillaries we used had no covalently attached coating, they could not necessarily be considered completely uncoated. Belder and Schomburg showed that the physical adsorption of HEC (present in the buffer) on bare fused-silica capillary walls improved CE separation efficiency by considerably improving peak symmetry and the width of peaks relative to migration times [93]. They determined that this physical adsorption of HEC created a "dynamic" coating, partially suppressing electroosmosis, and preventing adsorption of analytes on the capillary walls. Smith and Rassi [94] determined that capillaries which were specially coated with the goal of achieving relatively strong and constant electroosmotic flow were useful for high-efficiency separations of biopolymers. We find that with consistent and careful pre-run treatment of the capillary with sodium hydroxide, we were also able to achieve the same strong and constant electroosmotic flow which they found to be useful.

Each new, uncoated capillary was treated with 1 M NaOH for 3 h before putting it to use, to etch the fused silica surface completely clean of adsorbed impurities. Insufficiently etched capillaries gave broad DNA peaks, although the peak for the neutral marker remained sharp. We attribute this to the attraction of DNA fragments to cations adsorbed onto the silica wall. After the initial 3 h treatment with 1 M NaOH, short treatments with base between runs sufficed to clean out the previous buffer/HEC mixture and refresh the necessary wall condition for excellent separations. In the electropherograms, peaks were identified by integration of peak areas. All four DNA bases (adenine, thymine, guanine, cytosine) absorb UV light [95]; thus, the UV absorbance peak area of a separated peak is proportional to the number of base pairs in the DNA molecules in that peak. A representative plot of peak area *vs.* number of DNA base pairs is shown in our most recent paper [48].

3 Results and discussion

3.1 The electrophoretic mobility of DNA as a function of HEC concentration (M_n 27000)

In the present study, we determined the mobility of double-stranded DNA restriction fragments ranging in size from 72 bp to 23130 bp as a function of HEC concentration for HEC of two different lengths. In previous work [48], we used viscosity measurements to determine the overlap threshold concentrations of these HEC samples: for HEC (M_n 27000), $\Phi^* \approx 1.80\%$ w/w, while for HEC (M_n 105000), $\Phi^* \approx 0.37\%$ w/w.

We have previously shown that solutions of low-molecular weight HEC (M_n 27000) do not have the ability to separate the larger fragments in a ΦX174-*Hae*III restriction digest (872, 1078, and 1353 bp) very well even at the low concentrations which favor resolution of large DNA [48]. Figure 1a depicts the CE of restriction fragments up to 23.1 kbp in length in a 0.30% w/w solution of HEC (M_n 27000). We found that 0.30% w/w is roughly the optimum HEC (M_n 27000) concentration to separate DNA larger than 1 kbp, yet still these larger fragments cannot be separated with baseline resolution, at least with our detection system. This illustrates the relative uselessness of low-molecular weight cellulose polymers for the separation of DNA larger than 1 kbp. Figure 1b shows the separation of ΦX174-*Hae*III restriction fragments in 0.90% w/w HEC (M_n 27000). Increased HEC concentration results in poorer resolution of the three largest DNA fragments in the ΦX174-*Hae*III digest than that achieved at 0.30% w/w HEC. While resolution of the smaller DNA fragments does improve markedly as HEC concentration is increased, 10-bp resolution of the 271 bp/281 bp fragments cannot be achieved using this low-molecular weight HEC. At 3.0% w/w HEC (M_n 27000), the solution becomes impractically viscous for

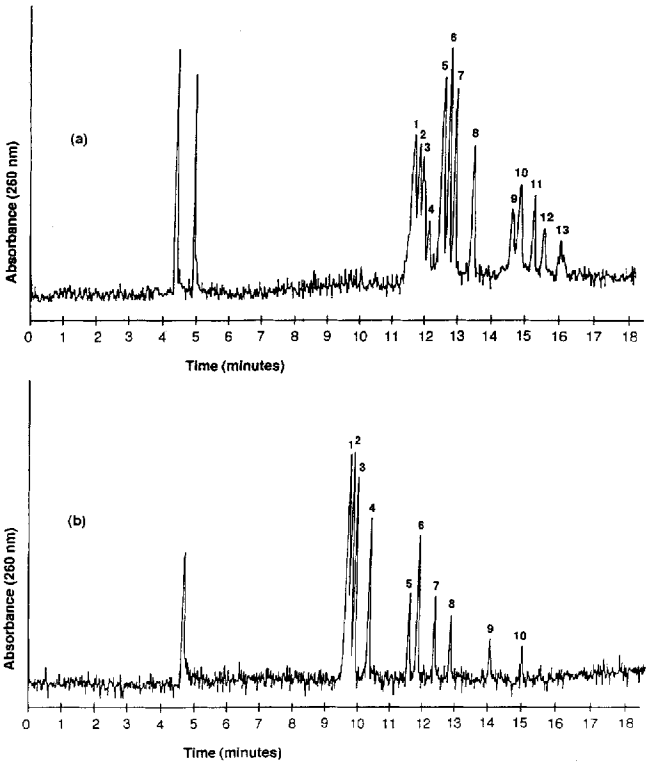

Figure 1. Separation by capillary electrophoresis of λ-*Hin*dIII and ΦX174-*Hae*III restriction fragments (in nonstoichiometric mixture) (a) in 0.30% w/w HEC (M_n 24000–27000). The far left peak corresponds to a neutral marker (mesityl oxide), used to determine the velocity of electroosmotic flow in the capillary, while the second peak at left is an impurity present in the DNA sample. Peak identification: (1) 23130 bp, (2) 9416 bp, (3) 6557 + 4361 bp, (4) 2322 + 2027 bp, (5) 1353 bp, (6) 1078 bp, (7) 872 bp, (8) 603 bp, (9) 310 bp, (10) 281 + 271 bp, (11) 234 bp, (12) 194 bp, and (13) 118 + 72 bp. λ-*Hin*dIII restriction fragments of 125 bp and 564 bp are present in such small concentrations that they are too faint to be seen. (b) in 0.90% w/w HEC (24000–27000). The far left peak corresponds to a neutral marker (mesityl oxide). Peak identification: (1) 1353 bp, (2) 1078 bp, (3) 872 bp, (4) 603 bp, (5) 310 bp, (6) 281 + 271 bp, (7) 234 bp, (8) 194 bp, (9) 118 bp, and (10) 72 bp. Peaks were identified by integration of peak area (see [48] for a sample plot). Buffer: 89 mM Tris, 89 mM boric acid, 5 mM EDTA pH 8.15. Capillary: 51 μm ID, 50 cm total length (35 cm to detector); temperature, 30 ± 0.1°C. Detection was by UV absorbance at 260 nm. Injection was hydrodynamic. Electrophoresis conditions: field strength 265 V/cm, current (a) 8.0 μA, (b) 9.6 μA. RSD of absolute electrophoretic mobilities: (a) 0.22%, $n = 4$; and (b) 0.30%, $n = 5$.

hydrodynamic filling and injection. Furthermore, at this concentration the three largest DNA fragments eluted as one poorly shaped peak, and appeared to have anomalously low mobilities, as though they were becoming trapped in the HEC matrix while the smaller fragments were not. This can be seen clearly in Fig. 2a, which is a plot of DNA electrophoretic mobility *vs.* HEC concentration (M_n 27000). The mobilities of the larger restriction fragments (> 603 bp) are so close on this plot as to be indistinguishable, although the peaks can be clearly discerned in Fig. 1a and 1b. However, if one follows the smooth curve of the data in Fig. 2a for the 1353/1078/872 bp fragments, a sudden drop in mobility can be seen at 3.0% w/w HEC. Although the measured overlap threshold concentration for HEC (M_n 27000 is ≈ 1.80% w/w [48], the only discernible change in the mobility data observed at or near this concentration is the complete loss of resolution for the three largest DNA fragments (872, 1078, and 1353 bp). It is clear, therefore, that entanglement of the HEC chains with each other is not an important factor in achieving DNA separations, and may in fact even be detrimental to the resolution of larger fragments. Furthermore, low-molecular weight HEC polymers are not effective for separations of DNA larger than 1 kbp, although relatively poor resolution may be achieved at low concentrations.

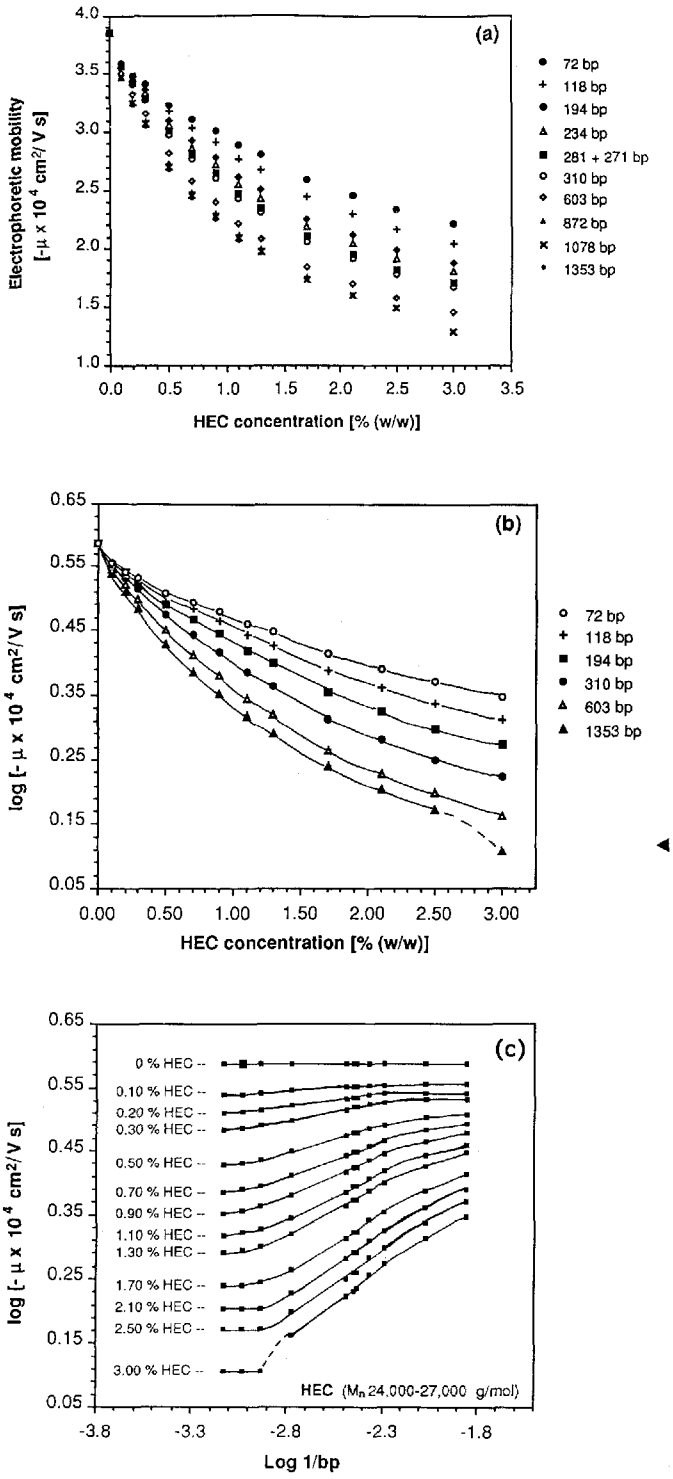

To test the applicability of both the original and the extended Ogston model to this data, a Ferguson plot for six DNA fragments ranging in size from 72 to 1353 bp is depicted in Fig. 2b. Lines are drawn through the data to guide the eye. The data for all fragments follow a smooth concave curve, with the amount of curvature increasing as DNA size increases. Even for the small 72 bp fragment, however, the data is clearly curved, especially at low HEC (M_n 27000) concentrations. From this plot, it is apparent that the original Ogston model does not describe DNA electrophoretic mobility in solutions of this low-molecular weight HEC, since it predicts that this data will form a straight line. The extended Ogston model [72–74], which is designed to fit curved Ferguson plots, could likely be made to fit these data. However, the basic geometrical assumptions of the extended Ogston model are the same as for the original Ogston model, *i.e.*, an infinite network of long, straight fibers. There is reason to doubt that these basic physical assumptions of the Ogston model are reasonable at low HEC concentrations. For example, DNA separation takes place in uncrosslinked HEC solutions at concentrations as low as 0.10% w/w HEC (M_n 27000), although these HEC polymers only form an entangled network

◀ *Figure 2.* (a) A plot of DNA electrophoretic mobility *vs.* HEC concentration (M_n 24000–27000) for DNA restriction fragments ranging from 72 bp to 23130 bp in length. Data points at each HEC concentration are the average of 3–5 individual determinations. Average run-to-run variation in calculated electrophoretic mobilities: ± 0.33%. DNA electrophoretic mobility was calculated by subtracting the electroosmotic mobility, calculated from the elution time of a neutral marker, from the apparent electrophoretic mobility of the DNA fragments, as DNA electrophoretic motion was opposite in direction to the electroosmotic flow which was used to drive it past the UV absorbance detector. The electrophoresis buffer, all conditions, and DNA sample, same as in Fig. 1. (b) A Ferguson plot of the data shown in (a), for six representative DNA fragments in the ΦX174-*Hae*III restriction digest. Lines are drawn through the data only to guide the eye. This plot is generally used to test the applicability of the Ogston model for electrophoresis data. According to the original Ogston model, the data for each DNA fragment should form a straight line, especially at low HEC concentrations. (c) A plot of the logarithm of the absolute mobility of 11 DNA fragments (ranging in size from 72 bp to 1353 bp) *vs.* the logarithm of inverse molecular size (in bp), for thirteen different concentrations of HEC (M_n 27000 g/mol). Lines are drawn through the data only to guide the eye. This plot is generally used to test the applicability of the reptation model. A dashed line is drawn through the mobility data of larger DNA fragments (872–1353 bp) at high HEC concentration (3.00% w/w) because these fragments eluted as a single poorly shaped peak with an anomalously low mobility.

above ~ 1.80% w/w [48]. Thus, separation takes place in dilute solutions in which no "network" is likely to exist, only nonentangled, noninteracting HEC polymers in random-coil conformations. Furthermore, the data form smooth, continuous curves over the entire concentration range studied, both well below and well above the overlap threshold. This suggests that the mechanism of DNA separation is the same at all HEC concentrations, and is not the Ogston mechanism.

To test the applicability of the reptation model [69, 75, 76] to this data, we plot the logarithm of the absolute electrophoretic mobility as a function of the logarithm of inverse molecular size (in bp) in each DNA fragment. The mobility data is not extrapolated back to zero field strength, as would be required to rigorously test the theoretical model of Slater *et al.* [69], which assumes low electric fields. This means that the effects of DNA stretching and orientation on the mobility are reflected in the plot. However, it is interesting to see what these effects are on the shape and slope of this plot which has been an important tool in the interpretation of DNA electrophoresis data [69]. It is thought the reptation (without DNA stretching) model applies in the linear region of this plot, which is expected theoretically to have a slope of −1.0. This behavior has been observed experimentally for the electrophoresis of DNA in slab gels (*e.g.*, [69, 78]). Figure 2c shows this "reptation plot", in which data is plotted for thirteen different HEC (M_n 27000) concentrations, and lines are drawn through the data only to guide the eye. Recall that the overlap threshold for this HEC sample in TBE buffer is about 1.80% w/w; thus, much of the electrophoresis data shown in Fig. 2c was taken at concentrations well below Φ^*. The data have a region which is somewhat linear for DNA ranging in size from 194 bp to 310 bp (the region in the center of the curves, where log 1/bp is between about −2.3 and −2.8). This is an extremely narrow linear region, compared to that observed in gels, where the reptation model applies for DNA from a few hundred to several thousand base pairs in length [69, 75, 76]. Furthermore, the slope of this so-called "linear region" of the plot ranges only from 0 (for 0% w/w HEC) to −0.26 (for 3.0% w/w HEC). From these results we conclude that (i) the data shown in Fig. 2c do form continuous curves, and (ii) the reptation model does not fit these curves. In Fig. 2c, a dashed line is drawn through the mobility data of larger DNA fragments (872–1353 bp) at high HEC concentration (3.00% w/w because these fragments eluted as a single poorly shaped peak with an anomalously low mobility.

3.2 The electrophoretic mobility of DNA as a function of HEC concentration (M_n 105000)

We have demonstrated that DNA separation is possible in uncrosslinked polymer solutions with concentrations well below the HEC overlap threshold (Φ^*) [48], experimentally confirming the theoretical prediction of Viovy and Duke [60]. For example, an excellent separation of ΦX174-*Hae*III restriction fragments was obtained in a 0.09% w/w HEC (M_n 105000) solution, although the measured overlap threshold of this longer HEC is ≈ 0.37% w/w [48]. Here, we test the usefulness of this HEC sample further, attempting to separate larger DNA restriction fragments, and determining the minimum HEC (M_n 105000) concentration required for DNA separation. Figure 3a depicts the separation by CE of a mixture of Φ174-*Hae*III and λ-*Hin*dIII DNA restriction fragments, ranging between 72 bp and 23.1 kbp, in a 0.15% w/w HEC (M_n 105000) solution. Clearly, this longer HEC provides better resolution of large DNA restriction fragments than HEC (M_n 27000), as well as partial resolution of the 271 and 281 bp fragments. With a more sensitive detection system, such as laser-induced fluorescence, smaller sample volumes could be used and the 271 and 281 bp fragments would likely be resolved to baseline. Figure 3b shows the separation of the same restriction digest in a 0.025% w/w HEC (M_n 105000) solution. At this concentration, resolution is essentially lost for DNA smaller than 603 bp, but retained for the larger restriction fragments. Even at concentrations as low as 0.00125% w/w (12 parts per million) resolution of DNA fragments larger than 2 kbp is achieved (see Fig. 3c). Resolution is only completely lost when HEC concentration is reduced below 1.56 parts per million, at which concentration the restriction fragments only separate into two large peaks (Fig. 3d). In free solution, all of the DNA fragments eluted as one peak.

In most of the electropherograms, the peak for the largest DNA fragment (23130 bp) was asymmetrically shaped, as seen in Fig. 3a–c. It appears from this peak shape that unlike smaller DNA fragments, the 23.1 kbp molecules have a fairly broad distribution of mobilities. Although the majority of the 23.1 kbp molecules migrate at a single mobility, (giving the peak its high, sharp right edge), others have a distribution of slower mobilities. This reduction in absolute mobility could be related to entanglement interactions with the HEC polymers, or perhaps to nonspecific physical adsorption of the long DNA on the capillary walls. This unsymmetric peak shape has also been observed by others who have separated λ-*Hin*dIII DNA restriction fragments in uncrosslinked cellulosic polymer solutions, employing coated capillaries [36, 46]. Interestingly, Chiari *et al.* [44] have used coated capillaries to separate the λ-*Hin*dIII DNA restriction fragments in a viscous solution of 4.5% uncrosslinked polyacrylamide, and obtained nicely symmetric peak shapes even for the largest 23 kbp DNA fragment.

Figure 4a gives a plot of DNA electrophoretic mobility (μ) as a function of HEC (M_n 105000) concentration for this mixture of ΦX174-*Hae*III and λ-*Hin*dIII restriction fragments. Although the measured overlap threshold concentration of this HEC (M_n 105000) is ≈ 0.37% w/w, the only distinguishable change in the mobility data at or near this concentration is the rapid loss in resolution of DNA larger than 603 bp. From this plot it is apparent that the larger DNA restriction fragments (603 bp–23.1 kbp) are best separated at *low* HEC concentrations, below the overlap threshold. Indeed, we observed that at higher concentrations, such as 0.55% w/w, the largest DNA peaks begin to merge and peak shape severely degrades (data not shown). This finding is in direct contradiction to the theoretical prediction of Viovy and

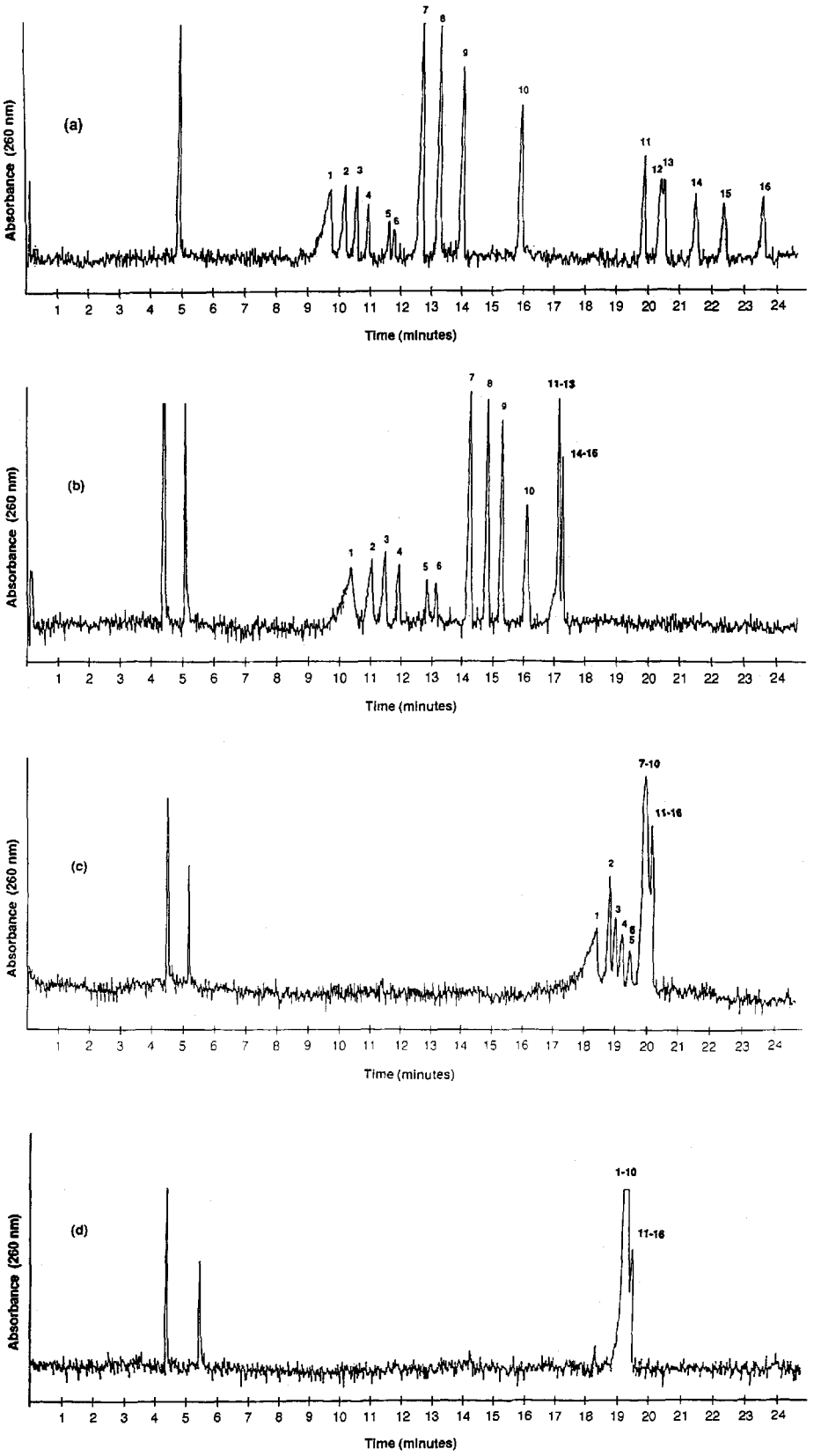

Figure 3. CE separation of λ-*Hin*dIII and ΦX174-*Hae*III restriction fragments (in nonstoichiometric mixture): (a) in 0.15% w/w HEC (M_n 90000–105000). The far left peak corresponds to a neutral marker (mesityl oxide), used to determine the velocity of electroosmotic flow in the capillary. Peak identification: (1) 23130 bp, (2) 9416 bp, (e) 6557 bp, (4) 4361 bp, (5) 2322 bp, (6) 2027 bp, (7) 1353 bp, (8) 1078 bp, (9) 872 bp, (10) 603 bp, (11) 310 bp, (12) 281 bp, (13) 271 bp, (14) 234 bp, (15) 194 bp, (16) 118 + 72 bp. λ-*Hin*dIII restriction fragments of 125 bp and 564 bp are present in such small concentrations that they are too faint to be seen. (b) In 0.025% w/w HEC (M_n 90000–105000). The far left peak corresponds to a neutral marker (mesityl oxide), while the second peak at left is an impurity present in the DNA sample. Peak identification: same as (a). (c) In 0.00125% w/w HEC (M_n 90000–105000). The far left peak corresponds to a neutral marker (mesityl oxide), while the second peak at left is an impurity present in the DNA sample. Peak identification: same as (a). (d) In 0.00015625% w/w HEC (M_n 90000–105000) (this extremely low concentration was obtained by successive dilution). The far left peak corresponds to a neutral marker (mesityl oxide), while the second peak at left is an impurity present in the DNA sample. Peak identification: same as a). Peaks were identified by integration of peak areas (see [48] for a sample plot). Electrophoresis conditions: current (a) 8.5 μA, (b) 7.2 μA, (c) 7.2 μA, (d) 7.2 μA. Other details as in Fig. 1. RSD of absolute electrophoretic mobilities: (a) 0.32%, n = 3; (b) 0.41%, n = 5; (c) 0.28%, n = 3; (d) 0.07%, n = 3.

Duke [60], who anticipated from their calculations that it would be necessary to raise the polymer concentration above some minimal value, significantly higher than the entanglement threshold Φ^*, in order to separate large DNA molecules. Viovy and Duke further predicted that, for a given high molecular weight polymer, the size of the largest DNA that can be separated should increase roughly linearly with the viscosity of the polymer solution. Clearly, this is not the case; in fact, we find the opposite to be true (*i.e.*, the larger DNA is best separated in dilute, low-viscosity solutions). Smaller DNA, on the other hand, is best resolved in more concentrated solutions.

Note that for fragments larger than 2 kbp, there is a distinct concave curvature in Fig. 4a at low HEC concentrations. Figure 4b shows the ultradilute solution data on an expanded scale; the transition from the equal electrophoretic mobilities of all DNA fragments in free solution, to size-dependent electrophoretic mobilities, is seen to occur at a concentration of about 6 ppm. Note that at the low concentrations depicted on Fig. 4b, all DNA restriction fragments smaller than 872 bp migrate with the same electrophoretic mobility.

At concentrations two orders of magnitude below the overlap threshold, HEC chains remain relatively isolated in solution. Although chains collide and interact transiently, HEC does not form an entangled network. Nothing resembling the "tubes" or "pores", which are assumed to exist in the reptation model, would be expected to exist here. The Ogston and extended Ogston models both assume the existence of an infinite network of crossed linear fibers. Once again, in ultradilute HEC solutions a polymer network such as this would not be expected to exist. Yet, DNA larger than 2 kbp can be

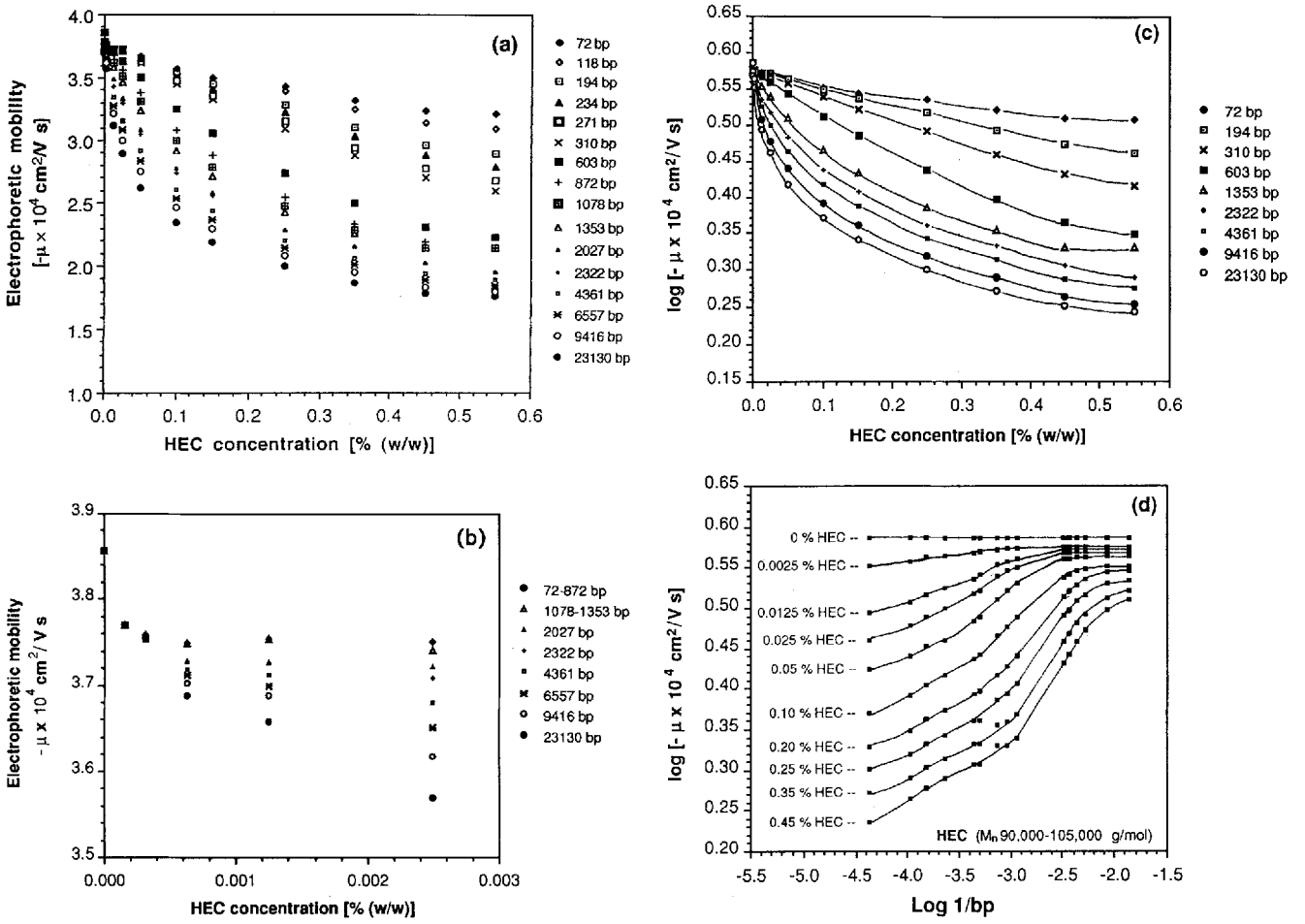

Figure 4. (a) A plot of DNA electrophoretic mobility *vs.* HEC concentration (HEC M_n 90 000–105 000 g/mol) for DNA restriction fragments ranging from 72 bp to 23130 bp in length, normal scale. (b) The same data plotted on an expanded scale to show detail at extremely low HEC concentrations. Data points at each HEC concentration are the average of 3–5 individual determinations. Average run-to-run variation in calculated electrophoretic mobilities: ± 0.46%. DNA electrophoretic mobility was calculated by subtracting the electroosmotic mobility, calculated from the elution time of a neutral marker, from the apparent electrophoretic mobility of the DNA fragments, as DNA electrophoretic motion was opposite in direction to the electroosmotic flow which was used to drive it past the UV absorbance detector. The electrophoresis buffer, all conditions, and DNA sample, same as in Fig. 1. (c) A Ferguson plot of the data shown in (a), for nine representative λ-*Hin*dIII and ΦX174-*Hae*III restriction fragments. Lines are drawn through the data only to guide the eye. This plot is generally used to test the applicability of the Ogston model for electrophoresis data. According to the original Ogston model, the data for each DNA fragment should form a straight line, especially at low HEC concentrations. (d) A plot of the logarithm of the absolute mobility of 16 DNA fragments (ranging in size from 72 bp to 23130 bp) *vs.* the logarithm of inverse molecular size (in bp), for ten different concentrations of HEC (M_n 90 000–105 000 g/mol). Lines are drawn through the data only to guide the eye. This plot is generally used to test the applicability of the reptation model.

readily separated at these concentrations. This suggests that the mechanism of DNA separation in dilute, uncrosslinked polymer solutions must be quite different from that postulated for agarose and polyacrylamide gels. In an extremely dilute, uncrosslinked polymer solution, no obstacle is permanent on the time scale of DNA motion [96]. As proposed by Bode in 1979 [80], the controlling factor in DNA electrophoretic mobility would most likely be the local resistance of polymer chains to dislocation and deformation, which would depend on the relative sizes of the DNA and the polymer chains, as well as polymer properties such as stiffness.

The original Ogston model of DNA electrophoresis [65–68, 97] assumes that DNA moves as an undeformable sphere through a random fiber matrix with a certain average pore radius, diffusing laterally until it encounters a pore large enough in radius and having a large enough volume to accommodate its passage. The extended Ogston model [72–74, 98] relies upon the same basic geometrical assumption. Yet, as we have pointed out, we find separation to be possible when no "pores", or even a polymer network, could exist. The original Ogston model also predicts that a Ferguson plot will be a straight line at low HEC concentrations with a slope equal to the retardation coefficient, K_r, which is a function of the gel fiber radius and DNA radius of gyration. The extended Ogston model allows K_r to vary with the gel concentration as well, in order to allow a computer model to fit the nonlinear Ferguson plots which are typical for large DNA in both true gels and polymer solutions at moderate to high field strengths. Curvature of Ferguson plots with increasing gel or polymer concentration is explained, in the context of the extended Ogston model, by asuming that DNA stretches and elongates with increasing gel or polymer concentration, as it is forced to navigate through constrictive spaces in the random fiber network. Figure 4c is the Ferguson plot derived from the data in Fig. 4a for nine DNA fragments ranging from 72 bp to 23 bkp; lines are drawn through the data merely to guide the eye. This graph shows that the data clearly do not follow the original Ogston model (*i.e.*, a linear Ferguson plot is not obtained) for DNA larger than 600 bp, although the curvature is slight for very small DNA fragments. For DNA larger than 600 bp, the Ferguson plot is deeply curved at low concentrations. The extended Ogston model was proposed to describe the curvature of Ferguson plots, yet it can physically represent such curvature only when DNA stretching and deformation is favored (*i.e.*, at higher gel or polymer concentrations, when pores would be geometrically constrictive). According to this model, then, curvature should increase at higher polymer concentrations. However, we find for large DNA that the curvature *decreases* with increasing HEC concentration and is most pronounced at low HEC concentrations (< 0.2% w/w, Fig. 4c), when no such constrictive network would be expected to exist. From these results we conclude that neither the Ogston nor the extended Ogston model fit these data. We note that many papers have been published which use the extended Ogston model to fit and interpret data for CE (at relatively high fields) of large DNA in uncrosslinked polymer solutions [15–17, 42, 72–74, 99–101].

We also wished to test the applicability of the reptation model to this data for DNA electrophoresis in HEC (M_n 105 000). Accordingly, the traditional "reptation plot" is shown in Fig. 4d. Not surprisingly, this plot is qualitatively very similar to the reptation plot for the smaller HEC (Fig. 2c), although the data extend to much larger DNA sizes. One might be tempted to say that there is a linear region in the plot for DNA lengths between 872 bp and 2322 bp (the central region of Fig. 4d, where log 1/bp values are between −2.9 and −3.4). The slope of this "linear region" decreases from 0 (at 0% HEC) to about −0.125 for higher HEC concentrations. Clearly, then, the reptation model (which predicts a slope of −1.0) does not apply in this concentration range for these DNA fragments, at least under these high field strengths. In any case, the linear region is too narrow (872 bp–2333 bp) to be sensibly termed a "reptation regime". Based on this evidence, we conclude that the reptation model does not fit these DNA electrophoresis data for HEC (M_n 105 000) to any greater extent than it fit the data for HEC (M_n 27 000). Instead, the data form continuous, sigmoidal curves. We emphasize the fact that the overlap theshold for this HEC sample in TBE buffer is about 0.37% w/w [48]. Thus, most of the electrophoresis data shown in Fig. 4d was taken at concentrations well below the overlap threshold, where no rigid, entangled polymer network would exist to force the DNA to migrate through the constrictive "tubes" whose existence is assumed as a starting point for the theoretical calculations of the reptation model.

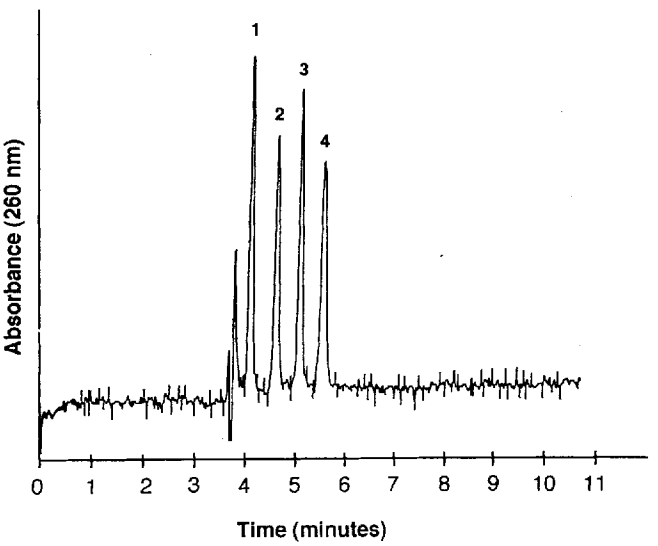

Figure 5. A representative electropherogram, showing the capillary electrophoretic separation of 4 negatively charged polystyrene latex spheres. Peaks were identified by spiking. The far left peak corresponds to a neutral marker, mesityl oxide. Peak identification: (1) sulfonated sphere, R = 61 nm; (2) carboxylated sphere, R = 29.5 nm; (3) sulfonated sphere, R = 116 nm; (4) sulfonated sphere, R = 132 nm. Note that the carboxylated spheres had a higher surface charge density than the three different sizes of sulfonated spheres (which had equal charge densities). Thus, although the radius of the carboxylated sphere is smaller than that of all sulfonated spheres, due to its different surface charge density it has an electrophoretic mobility intermediate between that of the two smaller sulfonated spheres. Buffer: 0.05 M sodium chloride, 0.05 M boric acid, 6 mM sodium hydroxide, pH 8.2, with 0.5% v/v Triton X-100 nonionic surfactant. Electrophoresis conditions: field strength 310 V/cm, current ~ 55 μA. Other details as in Fig. 1. % RSD of electrophoretic mobilities: 0.58%, n = 5.

3.3 Comparison of the electrophoretic behavior of negatively charged polystyrene latex spheres to that of DNA as a function of HEC concentration

In the Ogston model, the probability that a spherically coiled DNA molecule will fit through a given pore is assumed to be the basis for size separation. Since the basic premise of the model is that DNA molecules move as though they were spherical, we compared the electrophoretic behavior of charged polystyrene latex microspheres to that of DNA having a nearly equivalent radius of gyration. Figure 5 is a representative electropherogram showing the separation of the four sphere samples in 0.15% w/w HEC (M_n 105 000 g/mol); peaks were identified by spiking. Electrophoretic mobility data for the four sphere samples and for four DNA restriction fragments with similar radii are plotted together in Fig. 6a as a function of HEC concentration (for HEC M_n 27 000) and Fig. 6b as a function of HEC concentration (for HEC, M_n 105 000). It is immediately apparent that DNA behavior is quite different from that of the spheres. For DNA, both the net charge and the frictional coefficient scale as the number of base pairs [3]; hence, DNA electrophoretic mobility is independent of its length and it is not separated in free solution. Unlike DNA, charged spheres can be separated by free solution electrophoresis because the hydrodynamic drag on a sphere scales with the radius (R) by Stoke's Law, while the net charge scales with the surface area (R^2). Hence, electrophoretic mobility scales roughly as sphere radius, for spheres with equivalent surface charge densities. (Of the four sphere samples we used, the three sulfonated spheres have equal charge densities, while the carboxylated spheres have a higher charge density than the sulfonated spheres. Thus, although the radius of the carboxylated spheres is smaller than that of all sulfonated spheres, it has an electrophoretic mobility intermediate between that of the two smaller sulfonated spheres).

Originally, the basis for modeling DNA as a spherical coil was the fact that for both spheres and DNA, a straight line could be fit at low concentrations to a semilogarithmic plot of electrophoretic mobility *vs.* gel or polymer concentration (a Ferguson plot). For DNA, the slope of the Ferguson plot decreases with increasing concentration (concave curvature); this was taken to indi-

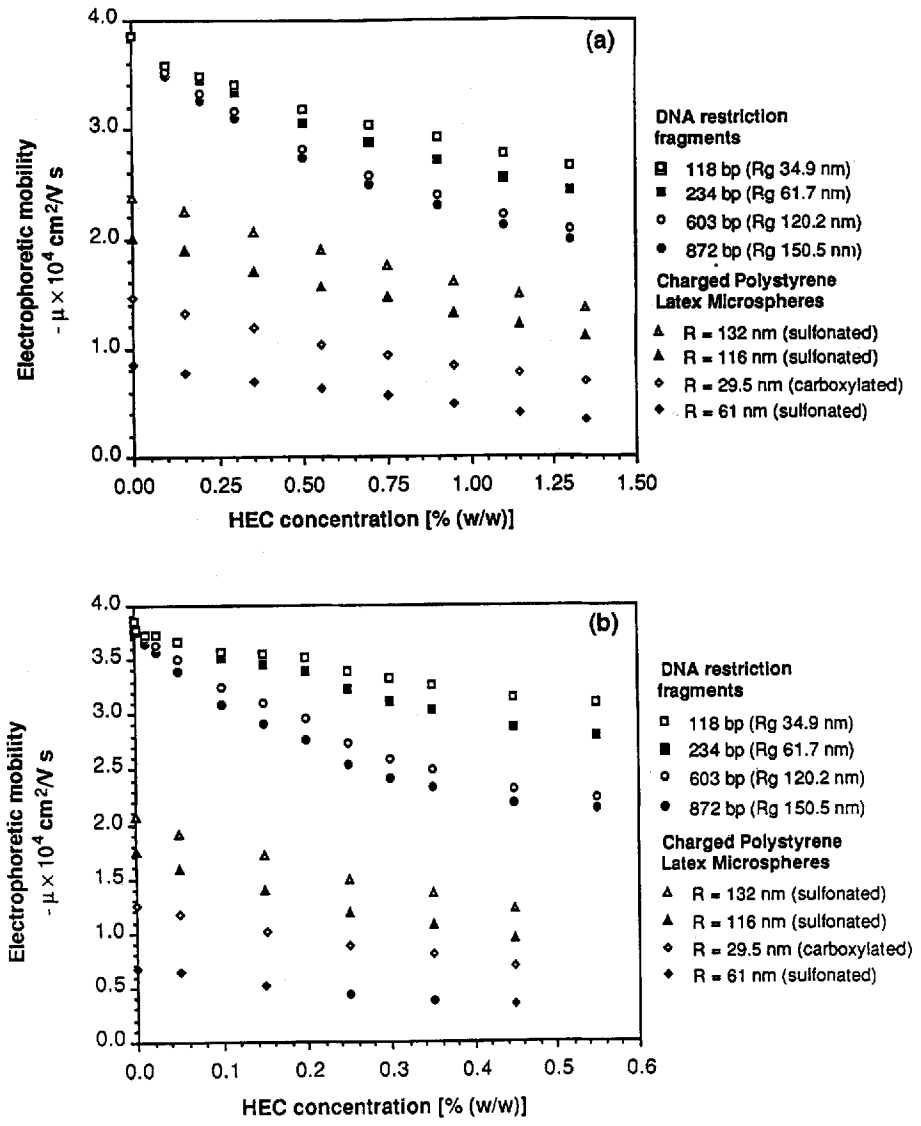

Figure 6. A comparison of the electrophoretic behavior of negatively charged polystyrene latex microspheres with that of DNA having similar radii of gyration, as calculated by the Porod-Kratky model for a stiff, worm-like coil [105]. Electrophoretic mobilities of both representative DNA restriction fragments and of the charged microspheres is plotted as a function of HEC concentration for HEC having a molecular mass of (a) 24 000–27 000 g/mol, and (b) 90 000–105 000 g/mol. Note that the carboxylated spheres have a higher surface charge density than the three sulfonated sphere samples (which have equal surface charge densities). Thus, although the carboxylated spheres have the smallest radius, their electrophoretic mobility is intermediate between that of the two smallest sulfonated spheres. Each data point on the graph is the average of 3–6 individual determinations. Average run-to-run % RSD of electrophoretic mobilities: (a) 0.93%, (b) 1.18%. Buffer, all electrophoresis methods and conditions, same as in Fig. 5. (c) A Ferguson plot of the data shown in (a), for the electrophoresis of four polystyrene latex microspheres in solutions of HEC (24 000–27 000 g/mol). (d) A Ferguson plot of the data shown in (b), for the electrophoresis of four polystyrene latex microspheres in solutions of HEC (90 000–105 000 g/mol).

cate that DNA deforms from its spherical conformation and "reptates" through the smaller "pores" which exist at high concentrations [82]. A Ferguson plot for sphere electrophoresis in a slab gel shows convex curvature at high gel concentrations [82]; the Ogston model has been fit to this data by allowing the radius of the gel fibers, one of the a parameters in the model, to vary with gel concentration [72, 73, 102, 103]. Figures 6c and 6d show the Ferguson plots for the four sphere samples we studied in HEC (M_n 27000) solutions and HEC (M_n 105000) solutions, respectively. The relationships are quite linear, except for the 61 nm sulfonated sphere data in Fig. 6c, which shows some convex curvature at high HEC concentrations. Thus, we observe the usual trends (*i.e.*, concave *vs.* convex curvature) in Ferguson plots for spheres and DNA in HEC solutions (Figs. 2c and 4d). We suggest that this fundamental, qualitative difference in DNA and sphere behavior indicates simply that the Ogston model is not appropriate for DNA electrophoresis in uncrosslinked polymer solutions.

One of the major reasons we chose to test the behavior of charged microspheres in uncrosslinked polymer solutions is that unlike DNA, a spherical particle cannot participate in entanglement interactions with the HEC polymers in the buffer. We believe such entanglement interactions to be the basis for DNA separation in dilute polymer solutions.

3.4 A transient entanglement coupling mechanism for DNA separation in polymer solutions

We propose an alternative mechanism of separation, different from those upon which the Ogston and reptation models of DNA electrophoresis are based. This proposed mechanism of separation is based on a consideration of the properties of HEC and DNA, as well as those of polymers in general. HEC is a linear (*i.e.*, nonbranched), uncharged cellulose derivative, having bulky ethylene oxide side chains terminating in hydroxyl groups. In aqueous solution, these hydrophilic side groups force HEC into a stiff, extended conformation. This stiffness is evidenced by a Porod-Kratky persistence length of 8.3 nm, roughly 10 times that of a typical flexible, random-coil polymer [104]. Double-stranded DNA is even stiffer

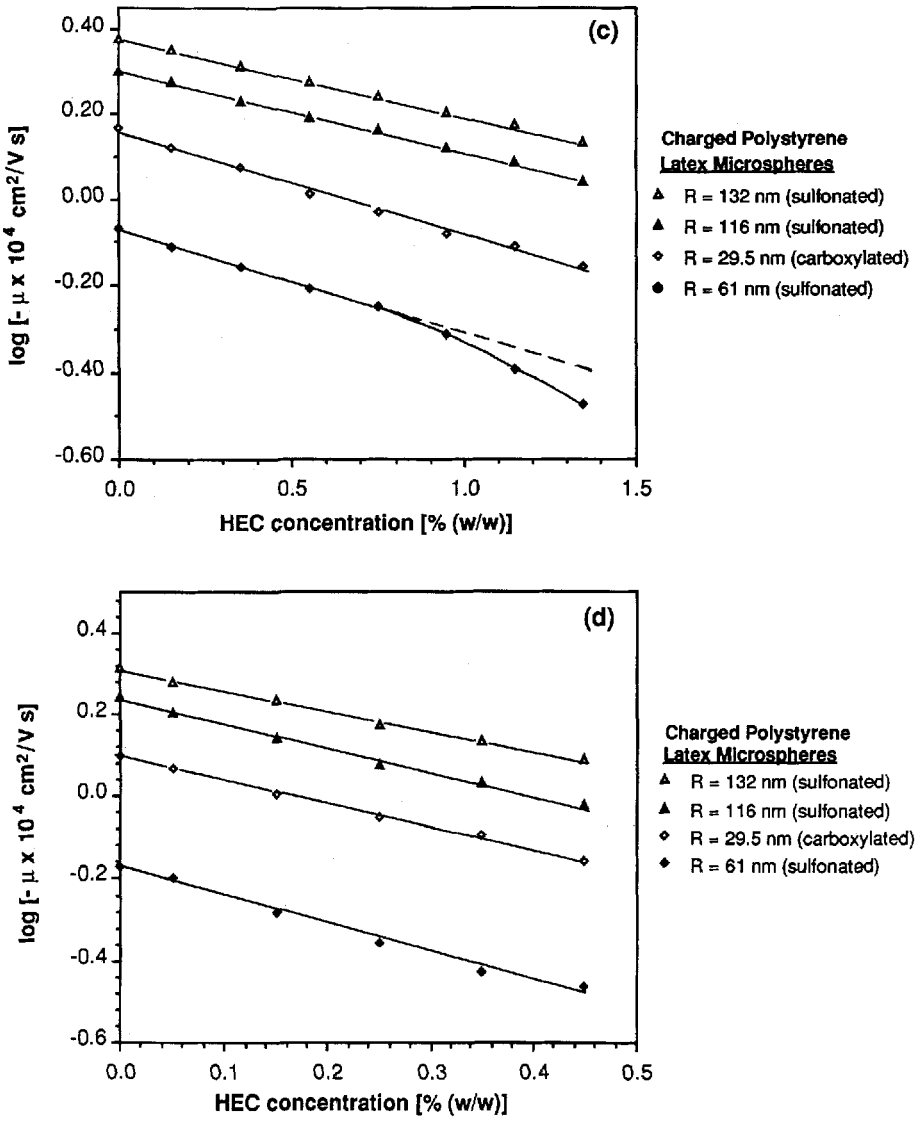

and more extended in solution than HEC, with a Porod-Kratky persistence length of 45 nm in 0.2 M buffer [105]. At comparable concentrations, stiff, extended polymers exhibit the effects of entanglement coupling much more strongly than flexible, random-coil polymers [106]. Given this, it is likely that when DNA molecules encounter isolated HEC molecules, they undergo transient entanglement coupling with HEC molecules, the effects of which are augmented by the stiffness of the two participants in the interaction. Hence, DNA molecules are forced to drag HEC molecules along with them, resulting in a decrease of DNA electrophoretic mobility. Larger DNA molecules have a higher probability of encountering and entangling with one or more HEC molecules. Figure 7 is a schematic illustration of DNA motion in dilute HEC solution, showing the relative sizes of large DNA (9461 bp) and small DNA (118 bp) compared to HEC (M_n 105000). In this figure, both DNA and HEC molecules are drawn with the correct number of properly scaled persistence lengths. As shown in the figure, large DNA has quite an open, free-draining conformation, allowing HEC chains to penetrate the DNA coil, increasing the probability of transient entanglement coupling. It has been demonstrated theoretically by Bueche that the molecular friction factor of a polymer in solution is much increased by entanglement coupling with other polymers [107]. Therefore, this type of DNA/HEC entanglement coupling interaction could alter the frictional characteristics of the DNA molecules moving under the influence of the electric field in a size-dependent manner. One of the advantages of this model for the mechanism of DNA separation is that it requires no theoretical constructs such as "pores" or "tubes".

Charged microspheres exhibit no improvement in their size separation as HEC concentration is increased (Fig. 6a and b). Based on our model, we suggest that this is because they are incapable of participating in transient entanglement coupling with the HEC molecules. The increased frictional drag the spheres experience in more concentrated, viscous solutions serves only to reduce their electrophoretic mobilities in such a way that they separate less well than in free solution, but no "pore network" exists to sieve them based on their size.

Using this model of DNA/HEC interactions, we can interpret the results we obtained with solutions of smaller HEC, having a number-average molecular weight in the range of 24000–27000 g/mol. We found that unlike the HEC with a molecular weight of 105000 g/mol, this smaller HEC does not have the ability to separate DNA larger than 603 bp very well even at low concentrations (Fig. 1a and b). This points to the fact that the relative sizes of the HEC and DNA molecules are important in size separation. Given the number-average molecular weights of the two HEC samples, we can use the average monomer molecular weight (272 g/mol) and the contour length per monomer (0.519 nm [104]) to determine the average total contour length of the HEC molecules. Using these quantities, the M_n 27000-HEC has a 51.5 nm contour length, while the M_n 105000-HEC has a contour length of 200.3 nm. Using the Porod-Kratky persistence length of HEC (8.3 nm) [104], we see that the shorter HEC has only 6.2 persistence lengths on average, while the larger HEC has about 24 persistence lengths. A molecule which is only able to bend at six places along its length will not entangle as strongly as a molecule which can bend in 24 places. Furthermore, when a larger HEC molecule is entangled with a DNA molecule, it causes more frictional drag than a smaller one. It seems likely that if the HEC molecules are too small, they may be too easily displaced by the larger DNA restriction fragments, because they form weak points of entanglement and are also too small to significantly hinder DNA electrophoretic motion. In this case, small HEC molecules would be less efficient in introducing size dependence to the molecular friction factor of larger DNA, as is observed experimentally.

3.5 Determination of the optimum HEC concentration to separate a given pair of restriction fragments

Using the data displayed in Fig. 2a and 4a, we may determine the optimum HEC concentration for the separation of each set of two adjacent DNA peaks, for each of

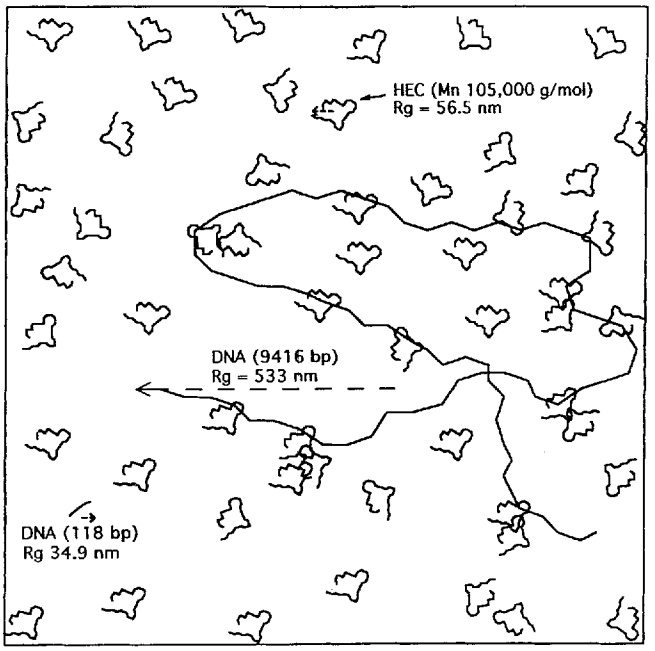

Figure 7. A schematic illustration of DNA motion in a dilute HEC solution. In the figure, the approximate relative sizes of HEC and small and large DNA are shown. Using the Porod-Kratky model for a stiff, worm-like coil [105], the calculated radius of gyration (R_g) of HEC (90000–105000 g/mol) is 56.5 nm. For a small, 118 bp DNA restriction fragment (from ΦX174-*Hae*III), the Porod-Kratky R_g is 35 nm, while the contour length is 40 nm. Since the Porod-Kratky persistence length of double-stranded DNA is 45 nm, this represents less than one persistence length and the 118 bp fragment is small and rod-like, and unlikely to entangle strongly with HEC in dilute solution. A larger DNA restriction fragment, consisting of 9416 bp (from λ*Hin*dIII) has a Porod-Kratky R_g of 533 nm; thus, it is ~ 10 times larger in radius than the HEC molecules. With a contour length of 3201 nm, this 9416 bp DNA fragment contains ~ 71 persistence lengths, as shown schematically in the figure, and has a high probability of undergoing transient entanglement coupling with many HEC molecules. When transient entanglement coupling occurs, the larger DNA molecule must drag the uncharged HEC molecules along with it during electrophoresis, decreasing its electrophoretic mobility in a size-dependent manner.

the two HEC samples used. This is accomplished by calculating the difference in DNA electrophoretic mobilities ($\Delta\mu$) for each set of adjacent peaks as a function of HEC concentration. Figure 8a is a plot of $\Delta\mu$ *vs.* HEC (M_n 27000) concentration for DNA ranging in size from 603 bp to 1353 bp. Lines are drawn through the data points merely to guide the eye. The HEC concentration at which the best peak separation is obtained increases with decreasing DNA size, contrary to the prediction of Viovy and Duke [60]. For example, the optimum concentration for resolving the 1353–1078 bp pair is $\approx$ 0.50% w/w HEC, while for the 1078–872 bp pair it is $\approx$ 0.70% w/w HEC, *etc.* Figures 8b and 8c depict $\Delta\mu$ values for the smaller DNA restriction fragments; it is clear that the smallest fragments require much higher HEC concentrations to reach their "optimum" peak separation. However, hydrodynamic filling and injection are no longer quick steps when such concentrated, viscous solutions of HEC (M_n 27000) are used, and in practice even the smallest fragments are sufficiently resolved in the concentration range 0.75–0.90% w/w.

For the larger HEC, we can determine optimum HEC concentrations to separate DNA as large as 23.1 kbp. Figures 9a and 9b give the plot of $\Delta\mu$ *vs.* HEC (M_n 105000) concentration for DNA ranging from 1353 bp to 23130 bp. Clearly, the optimum $\Delta\mu$ for these larger fragments is obtained at quite low HEC concentrations, in the range of 0.05 to 0.07% w/w HEC. Figure 9 (c) is the same plot for those DNA restriction fragments in the range 310 bp–1353 bp. Once again, the optimum HEC concentration for peak separation decreases with increasing DNA size. This may be because at higher concentrations randomly coiled DNA can no longer move easily through the solution, as the free space between HEC chains vanishes. At such high concentrations, the DNA may undergo a conformation change and become more elongated, such as is postulated to occur in the reptation model. In a rigid gel, a reptating DNA molecule encounters stiff obstacles and experiences frictional drag as it slides past these obstacles in an effective "tube". In an uncrosslinked polymer solution, the obstacles are easily dislocated as long as the solution is sufficiently dilute that a network is not established. Thus the reptating DNA molecule never encounters a truly stiff obstacle and is able to move rapidly through the solution in its elongated conformation. The easy dislocation of the HEC chains, in contrast to the semi-rigid structures of a

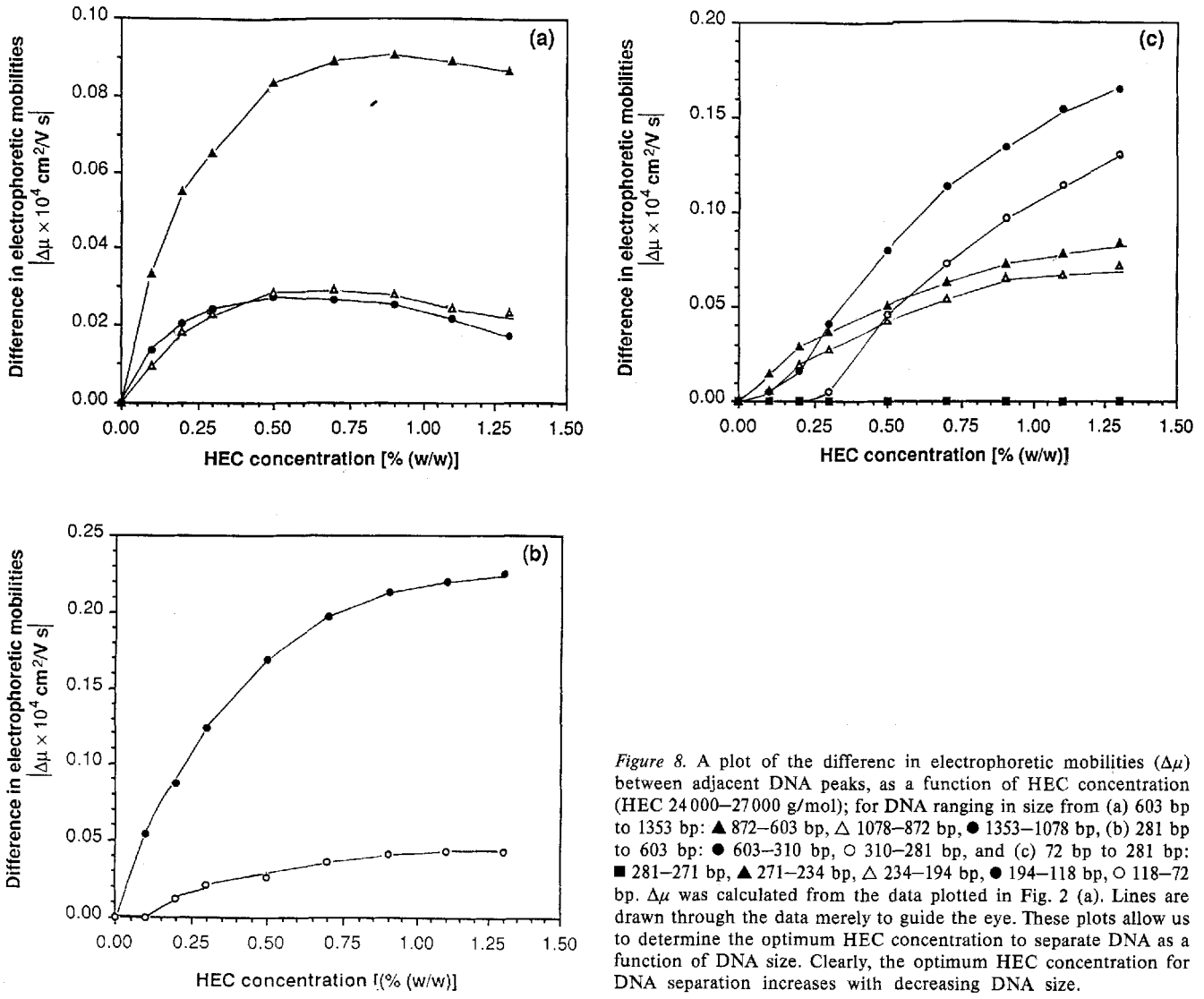

Figure 8. A plot of the differenc in electrophoretic mobilities ($\Delta\mu$) between adjacent DNA peaks, as a function of HEC concentration (HEC 24000–27000 g/mol); for DNA ranging in size from (a) 603 bp to 1353 bp: ▲ 872–603 bp, △ 1078–872 bp, ● 1353–1078 bp, (b) 281 bp to 603 bp: ● 603–310 bp, ○ 310–281 bp, and (c) 72 bp to 281 bp: ■ 281–271 bp, ▲ 271–234 bp, △ 234–194 bp, ● 194–118 bp, ○ 118–72 bp. $\Delta\mu$ was calculated from the data plotted in Fig. 2 (a). Lines are drawn through the data merely to guide the eye. These plots allow us to determine the optimum HEC concentration to separate DNA as a function of DNA size. Clearly, the optimum HEC concentration for DNA separation increases with decreasing DNA size.

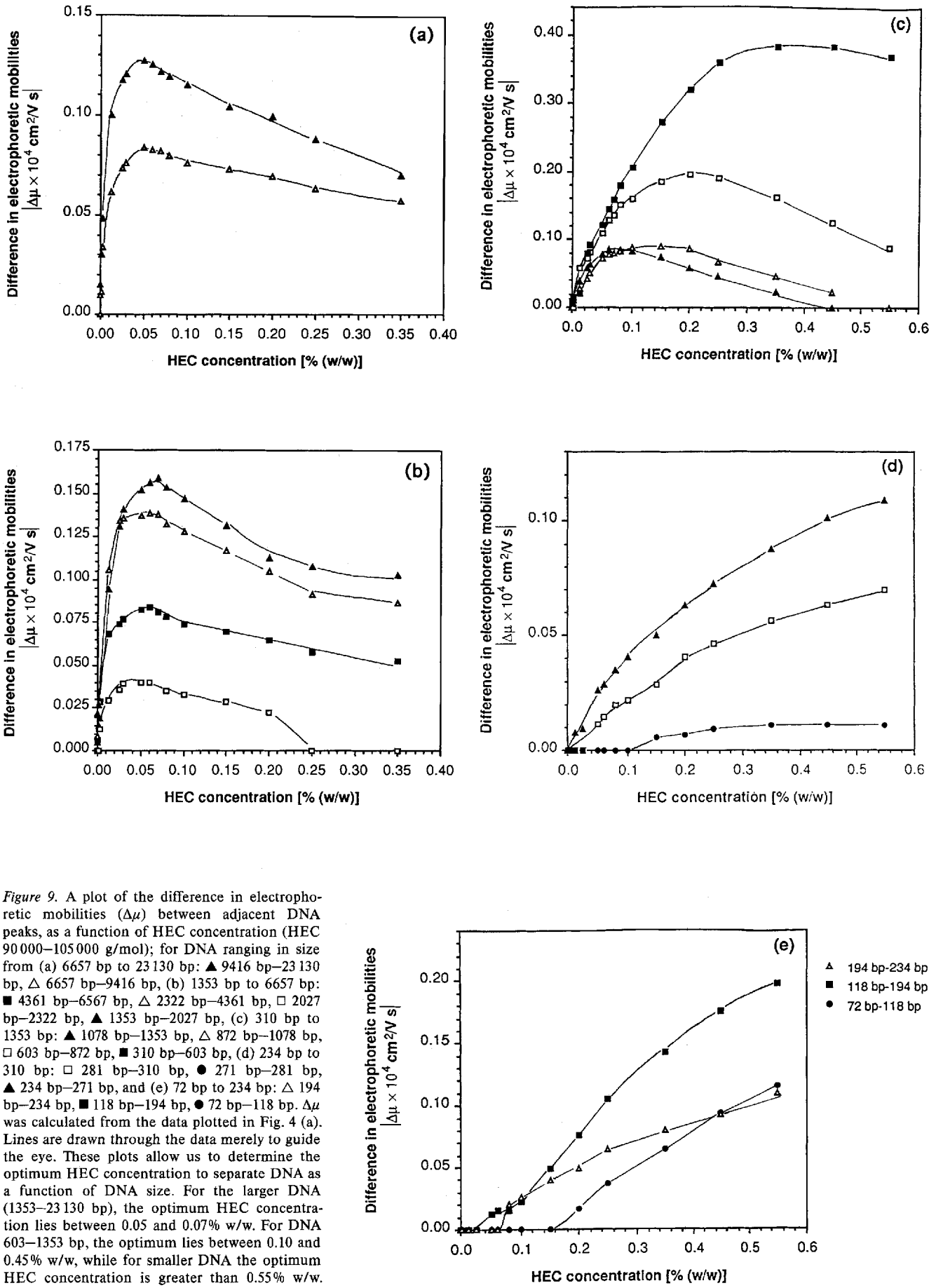

Figure 9. A plot of the difference in electrophoretic mobilities ($\Delta\mu$) between adjacent DNA peaks, as a function of HEC concentration (HEC 90 000–105 000 g/mol); for DNA ranging in size from (a) 6657 bp to 23 130 bp: ▲ 9416 bp–23 130 bp, △ 6657 bp–9416 bp, (b) 1353 bp to 6657 bp: ■ 4361 bp–6567 bp, △ 2322 bp–4361 bp, □ 2027 bp–2322 bp, ▲ 1353 bp–2027 bp, (c) 310 bp to 1353 bp: ▲ 1078 bp–1353 bp, △ 872 bp–1078 bp, □ 603 bp–872 bp, ■ 310 bp–603 bp, (d) 234 bp to 310 bp: □ 281 bp–310 bp, ● 271 bp–281 bp, ▲ 234 bp–271 bp, and (e) 72 bp to 234 bp: △ 194 bp–234 bp, ■ 118 bp–194 bp, ● 72 bp–118 bp. $\Delta\mu$ was calculated from the data plotted in Fig. 4 (a). Lines are drawn through the data merely to guide the eye. These plots allow us to determine the optimum HEC concentration to separate DNA as a function of DNA size. For the larger DNA (1353–23 130 bp), the optimum HEC concentration lies between 0.05 and 0.07% w/w. For DNA 603–1353 bp, the optimum lies between 0.10 and 0.45% w/w, while for smaller DNA the optimum HEC concentration is greater than 0.55% w/w.

gel, may effectively place the reptating DNA in a rapidly dilating tube which is constantly opening up to allow its passage. When the DNA migrates in this manner, the dependence of its frictional properties on molecular length would be decreased.

Figure 9d and 9e show $\Delta\mu$ *vs.* HEC concentrations for those fragments smaller than 310 bp; these small fragments have not yet reached their "optimum" even when the HEC (M_n 105 000) solution has reached a concentration of 0.55% w/w and is no longer practical for hydrodynamic filling and injection due to its high viscosity. However, at lower concentrations such as 0.20% w/w HEC (M_n 105 000), even the smallest DNA fragments (72 and 118 bp) are separated with excellent resolution, so it is not necessary to perform electrophoresis at the "optimum" HEC concentration. In practice, a value of $\Delta\mu$ greater than 0.05×10^4 cm^2/V s (see Fig. 8 and 9) will provide baseline resolution of the two DNA fragments of interest.

The "optimum" concentration most likely represents the concentration at which enough HEC molecules are present that the DNA of interest will have a high probability of entanglement coupling, yet at which the solution is not so concentrated that DNA is forced into an elongated, field-oriented conformation. This optimum concentration will be highly dependent on DNA and HEC length. In the same dilute solution (*e.g.*, 0.025% w/w HEC, Fig. 3b), a large DNA molecule (*e.g.*, 9416 bp) may be near this optimum concentration, while a much smaller DNA molecule (*e.g.*, 310 bp) is able to stream easily through the free space in the solution without encountering enough HEC molecules to provide good size-dependent drag. Bode introduced the concept of a microscopic viscosity [80] to model this effect, dividing a hypothetical polyacrylamide gel into low-viscosity regions, where no gel structures would be encountered, and high-viscosity regions, where a migrating macro-ion would encounter resistance to its electrophoretic motion.

Finally, we explicitly investigate the dependence of the optimum HEC concentration on DNA size, for both small and large HEC. Using the data shown in Fig. 8 and 9, we plot the optimum HEC concentration for the separation of two adjacent DNA peaks (*i.e.*, the HEC concentration at which the maximum $\Delta\mu$ is obtained) *versus* the number of base pairs in the "average" DNA molecule. The latter is calculated by adding the number of base pairs in the two DNA fragments which are separated and dividing by 2. The results of this correlation are shown in Fig. 10a for HEC with a molecular weight of 24 000–27 000 g/mol, and in Fig. 10b for HEC with a molecular weight of 90 000–105 000 g/mol. For Fig. 10a, we used data for the electrophoresis of a ΦX174-*Hae*III restriction digest, except for the 271 bp/281 bp fragments which this small HEC could not resolve at all. For Fig. 10b, we included data for both the ΦX174-*Hae*III and λ*Hin*dIII restriction fragments, with the exception of restriction fragments smaller than 281 bp. Even at the highest HEC concentration studied, $\Delta\mu$ for these smaller fragments had not yet approached a maximum. Therefore, we could not confidently estimate the optimum HEC concentration for separation.

The curves in Fig. 10a and 10b exhibit the same basic shape, reflecting the fact that, in general, the optimum HEC concentration for separation decreases monotonically with increasing DNA size. For small DNA fragments (less than 200 base pairs in M_n 27 000-HEC, less than 1000 bp in M_n 105 000-HEC), the optimum HEC concentration increases rapidly. The point at which the slope of the curve begins to approach infinity appears to be the concentration at which a transient entanglement coupling mechanism of separation ceases to be effective.

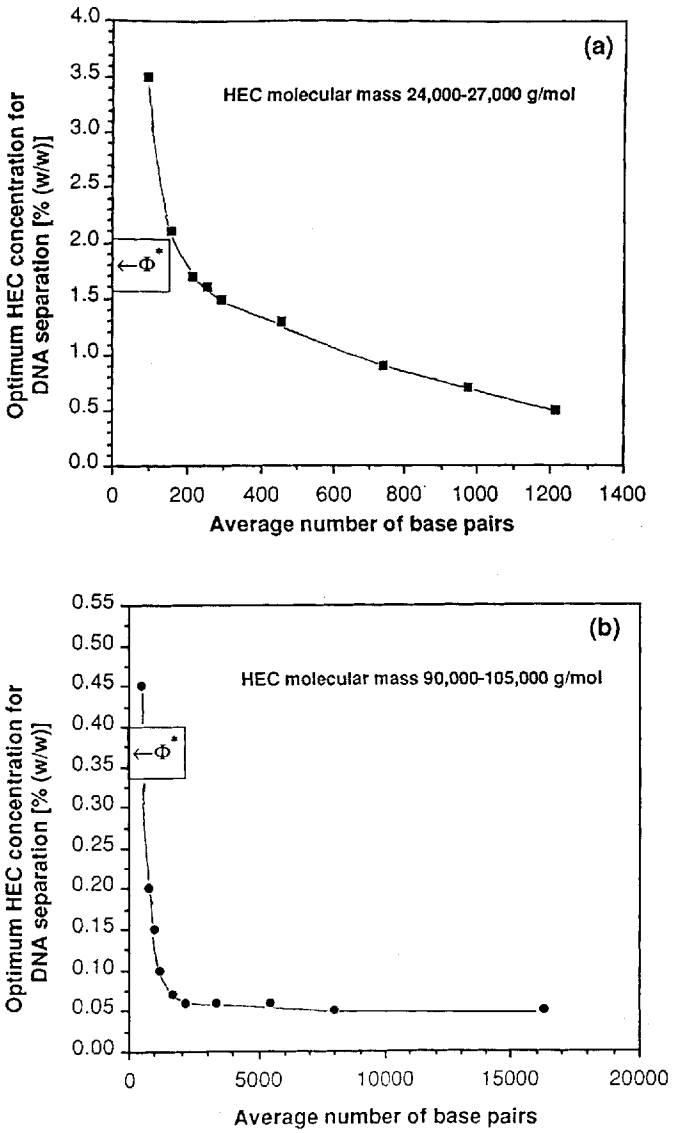

Figure 10. The optimum HEC concentration for DNA separation, plotted as a function of the length (in base pairs) of the "average" DNA molecule being separated, in solutions of (a) HEC 24 000–27 000 g/mol, and (b) HEC 90 000–105 000 g/mol. Each point represents the HEC concentration at which the largest difference in the electrophoretic mobilities of two similarly sized DNA restriction fragments is obtained (*i.e.*, the maximum $\Delta\mu$, as shown in Fig. 8 and 9). Lines are drawn through the data merely to guide the eye. The average number of DNA base pairs was calculated by adding the number of base pairs in the two similarly sized fragments and dividing by 2. Also shown on the plots are the overlap threshold concentration of these two HEC samples, *i.e.*, the concentration at which an entangled polymer network begins to form in solution (~ 1.80% w/w for HEC 24 000–27 000 g/mol, and ~ 0.37% w/w for HEC 90 000–105 000 g/mol) [48].

Given both the similarities and the differences in Fig. 10a and 10b, we propose that there are two requirements for successful DNA separation to occur by a transient entanglement coupling mechanism. First, the DNA molecules must be long enough to engage in true entanglement coupling. Second, the solution must be dilute enough that DNA molecules are able to move as random coils. Clearly, smaller DNA fragments, having only a few Porod-Kratky persistence lengths, require much more concentrated HEC solutions and many more contacts with HEC polymers to provide optimum size-dependent drag, since they are too short and stiff to undergo true "entanglement coupling". This seems to be an important factor for separation in M_n 27000 HEC (Fig. 10a), for the slope increases rapidly for DNA smaller than 200 bp (having less than 2 persistence lengths). However, this length requirement cannot be the only necessary factor for transient entanglement coupling, since the minimum DNA size apparently depends on the size of the HEC molecules. In M_n 105000 HEC (Fig. 10b), the slope increases rapidly for DNA smaller than 1000 bp. When a solution of M_n 105000 HEC becomes semidilute and approaches the overlap threshold concentration, DNA larger than 1000 bp, moving under the influence of a strong electric field, may be forced to adopt an elongated conformation. In this conformation, it would move essentially head-first. This is different from electrophoresis in dilute solution, in which the DNA chains retain a stiff, extended, and yet random conformation and present the maximum number of chain segments to passing HEC molecules for transient entanglement coupling. Furthermore, since DNA is a relatively free-draining polymer, HEC molecules can actually stream into large DNA coils to form points of entanglement there (as shown in Fig. 7). Thus, randomly coiled DNA has a high probability of entanglement coupling, and can be readily separated in dilute HEC solutions (*i.e.*, at concentrations which are below the HEC overlap threshold, Φ^*, as is pointed out in Fig. 10a and b). The fact that the most useful window of separation (the HEC concentration range which provides optimum separation of DNA ranging widely in size) occurs below Φ^* provides dramatic proof that the formation of a fully entangled network of the HEC polymers in the buffer is not generally advantageous for DNA separation by a transient entanglement coupling mechanism. The point at which the slope begins to approach infinity may also be the concentration at which the HEC matrix becomes confining, causing DNA to take on an elongated, field-oriented conformation, reducing the probability of transient entanglement coupling with HEC molecules.

4 Concluding remarks

The fact that DNA separations are achievable in ultradilute solutions of HEC suggests that a new approach must be taken to understand DNA motion in uncrosslinked polymer solutions, and that the models used for traditional gel electrophoresis are not appropriate. For example, the widely used Ogston model of DNA electrophoresis assumes that DNA moves as an unperturbed sphere through an infinite, random network of linear fibers which can be characterized by an "average pore size". We have compared the electrophoretic behavior of negatively charged latex microspheres to that of similarly sized DNA in HEC solutions, and found qualitatively different results for the two different types of analytes. We suggest that this difference in behavior is observed because the spheres are incapable of entangling with the HEC polymers. Furthermore, DNA is readily separated at concentrations so dilute that no "pores", or even an entangled polymer network, could exist. We consider this to be strong evidence that the sphere-based, polymer network-based Ogston model is not reasonable for DNA electrophoresis in dilute polymer solutions. Our data for DNA electrophoresis in uncrosslinked HEC solutions do not appear to fit the reptation model either. DNA electrophoresis experiments using solutions of HEC polymers which are relatively small (24000–27000 g/mol) and relatively large (90000–105000 g/mol) indicate that the number of HEC persistence lengths in the chain and the relative HEC/DNA sizes are important factors in resolution. Based on a transient entanglement coupling mechanism for DNA separation in dilute polymer solutions, we anticipate no *a priori* upper size limit to DNA which can be separated by CE in a constant field. In fact, at field strengths as high as those used in our CE experiments (265 V/cm) DNA as large as 23.1 kbp could not be separated in an agarose slab gel, which emphasizes that a different mechanism of separation is operative in this medium. It seems that using this CE technique, DNA larger that 23.1 kbp would simply require low concentrations of larger polymer molecules than those we have used to effect their separation. We are hopeful that we may achieve a dramatic speed increase in DNA restriction mapping separations of large DNA.

Received September 27, 1993

5 References

[1] Smith, C. L., Cantor, C. R., *TIBS* 1987, *12*, 284–287.
[2] Olivera, B. M., Baine, P., Davidson, N., *Biopolymers* 1964, *2*, 245–257.
[3] Lerman, L. S., Frisch, H. L., *Biopolymers* 1982, *21*, 995–997.
[4] Fangman, W. L., *Nucleic Acids Res.* 1978, *5*, 653–665.
[5] Schwartz, D. C., Cantor, C. R., *Cell* 1984, *37*, 67–76.
[6] Heller, C., Pohl, F. M., *Nucleic Acids Res.* 1989, *17*, 5989–6003.
[7] Maniatis, T., Fritsch, E. F., Sambrook, J., *Molecular Cloning: A Laboratory Manual*, Cold Spring Harbor Laboratory Press, Cold Spring Harbor, NY 1982.
[8] Brumley, R. L., Jr., Smith, L. M., *Nucleic Acids Res.* 1991, *19*, 4121–4126.
[9] Cohen, A. S., Paulus, A., Karger, B. L., *Chromatographia* 1987, *24*, 15–24.
[10] Cohen, A. S., Najarian, D. R., Paulus, A., Guttman, A., Smith, J. A., Karger, B. L., *Proc. Natl. Acad. Sci. USA* 1988, *85*, 9660–9663.
[11] Zhu, M., Hansen, D. L., Burd, S., Gannon, F., *J. Chromatogr.* 1989, *480*, 311–319.
[12] Heiger, D. N., Cohen, A. S., Karger, B. L., *J. Chromatogr.* 1990, *516*, 33–48.
[13] Guttman, A., Cohen, A. S., Heiger, D. N., Karger, B. L., *Anal. Chem.* 1990, *62*, 137–141.
[14] Liu, J., Dolnik, V., Hsieh, Y.-Z., Novotny, M., *Anal. Chem.* 1992, *64*, 1328–1336.
[15] Guszczynski, T., Pulyaeva, H., Tietz, D., Garner, M. M., Chrambach, A., *Electrophoresis* 1993, *14*, 523–530.
[16] Boček, P. and Chrambach, A., *Electrophoresis* 1992, *13*, 31–34.
[17] Pulyaeva, H., Wheeler, D., Garner, M. M., Chrambach, A., *Electrophoresis* 1992, *13*, 608–614.

[18] Chiari, M., Nesi, M., Fazio, M., Righetti, P. G., *Electrophoresis* 1992, *13*, 690–697.
[19] Lukacs, K. D., *Ph. D. Disseration,* University of North Carolina, Chapel Hill, NC 1983.
[20] Huang, X. C., Quesada, M. A., Mathies, R. A., *Anal. Chem.* 1992, *64*, 2129–2154.
[21] Albin, M., Chen, S.-M., Louie, A., Pairaud, C., Colburn, J., Wiktorowicz, J., *Anal. Biochem.* 1992, *206*, 382–388.
[22] Bruin, G. J. M., Wang, T., Xu, X., Kraak, J. C., Poppe, H., *J. Microcolumn. Sep.* 1992, *4*, 439–448.
[23] Altria, K. D., Dave, Y. K., *J. Chromatogra.* 1993, *633*, 221–225.
[24] Nashabeh, W., Smith, J. T., El Rassi, Z., *Electrophoresis* 1993, *14*, 407–416.
[25] Swerdlow, H., Gesteland, R., *Nucleic Acids Res.* 1990, *18*, 1415–1419.
[26] Drossman, H., Luckey, J. A., Kostichka, A. J., D'Cunha, J., Smith, L. M., *Anal. Chem.* 1990, *62*, 900–903.
[27] Yin, H. F., Lux, J. A., Schomburg, G., *J. High Resol. Chromatogr.* 1990, *13*, 624–627.
[28] Swerdlow, H., Wu, S., Harke, H., Dovichi, N. J., *J. Chromatogr.* 1990, *516*, 61–67.
[29] Luckey, J. A., Drossman, H., Kostichka, A. J., Mead, D. A., D'Cunha, J., Norris, T. B., Smith, L. M., *Nucleic Acids Res.* 1990, *18*, 4417–4421.
[30] Swerdlow, H., Dew-Jager, K. E., Grey, R., Dovichi, N. J., Gesteland, R., *Electrophoresis* 1992, *13*, 475–483.
[31] Cohen, A. S., Najarian, D. R., Karger, B. L., *J. Chromatorgr.* 1990, *516*, 49–60.
[32] Lux, J. A., Yin, H. F., Schomberg, G., *J. High Res. Chromatogr.* 1990, *13*, 436–437.
[33] Baba, Y., Matsuura, T., Wakamoto, K., Tsuhako, M., *Chem. Letters* 1991, 371–374.
[34] Baba, Y., Matsuura, T., Wakamoto, K., Morita, Y., Nishitsu, Y., Tsuhako, M., *Anal. Chem.* 1992, *64*, 1221–1225.
[35] Motsch, S. R., Kleemiß, M.-H., Schomburg, G., *J. High Res. Chromatogr.* 1991, *14*, 629–632.
[36] Chan, K. C., Whang, C.-W., Yeung, E. S. Y., *J. Liq. Chromatogr.* 1993, *16*, 1941–1962.
[37] Bode, H.-J., *FEBS Lett.* 1976, *65*, 56–58.
[38] Chin, A. M., Colburn, J. C., *Am. Biotech. Lab., News Edition* 1989, *7*, 16–16.
[39] Izumi, T., Yamaguchi, M., Yoneda, K., Isobe, T., Okuyama, T., Shinoda, T., *J. Chromatogr.* 1993, *652*, 41–46.
[40] Zhu, M., Hjertén, S., *European Patent Office Publication* No. 0 442 177 A1, 2/13/1990.
[41] Ganzler, K., Greve, K. S., Cohen, A. S., Karger, B. L., Guttman, A., Cooke, N. C., *Anal. Chem.* 1992, *64*, 2665–2671.
[42] Chrambach, A., Aldroubi, A., *Electrophoresis* 1993, *14*, 18–22.
[43] Paulus, A., Hüsken, D., *Electrophoresis* 1993, *14*, 27–35.
[44] Chiari, M., Nesi, M., Righetti, P. G., *J. Chromatogr.* 1993, *652*, 31–39.
[45] Schwartz, H. E., Ulfelder, K., Sunzeri, F. J., Busch, M. P., Brownlee, R. G., *J. Chromatogr.* 1991, *559*, 267–283.
[46] Strege, M., Lagu, A., *Anal. Chem.* 1991, *63*, 1233–1236.
[47] Grossman, P. D., Soane, D. S., *J. Chromatogr.* 1991, *559*, 257–266.
[48] Barron, A. E., Soane, D. S., Blanch, H. W., *J. Chromatogr.* 1993, *652*, 3–16.
[49] Kleemiß, M. H., Gilges, M., Schomburg, G., *Electrophoresis* 1993, *14*, 515–522.
[50] Singhal, R. P., Xian, J., *J. Chromatogr.* 1993, *652*, 47–56.
[51] MacCrehan, W. A., Rasmussen, H. T., Northrup, D. M., *J. Liq. Chromatogr.* 1992, *15*, 1063–1080.
[52] Maschke, H. E., Frenz, J., Belenkii, A., Karger, B. L., Hancock, W. S., *Electrophoresis* 1993, *14*, 509–514.
[53] McCord, B. R., Jung, J. M., Holleran, E. A., *J. Liq. Chromatogr.* 1992, *602*, 241–271.
[54] LePeq, J. B., *Methods Biochem. Anal.* 1971, *20*, 41–86.
[55] Guszczynski, T., Garner, M. M., Deml, M., Chrambach, A., *Appl. Theor. Electrophoresis* 1991, *2*, 151–157.
[56] Chrambach, A., Boček, P., Guszczynski, T., Garner, M. M., Geml, M., in: Radola, B. J. (Ed.), *Elektrophorese Forum '91*, Technical University Munich, 1991, pp. 35–51.
[57] Viovy, J.-L., Duke, T., *Electrophoresis* 1993, *14*, 322–329.
[58] de Gennes, P. G., *Scaling Concepts in Polymer Physics* Cornell University Press, Ithaca, NY 1979.
[59] Barnes, H. A., Hutton, J. F., Walters, K., *An Introduction to Rheology* Elsevier, Amsterdam 1989, Chapter 6.
[60] Viovy, J. L., Duke, T., *Electrophoresis* 1993, *14*, 322–329.
[61] Broseta, D., Leibler, L., Lapp, A., Strazielle, C., *Europhys. Lett.* 1986, *14*, 668–676.
[62] Righetti, P. G., *J. Biochem. Biophys. Methods* 1989, *19*, 1–20.
[63] Deutsch, J. M., *Science* 1988, *240*, 922–924.
[64] Smisek, D. L., Hoagland, D. A., *Science* 1990, *248*, 1221–1223.
[65] Ogston, A. G., *Trans. Faraday Soc.* 1958, *54*, 1754–1757.
[66] Rodbard, D., Chrambach, A., *Proc. Nat. Acad. Sci. USA* 1970, *65*, 970–977.
[67] Chrambach, A., Rodbard, D., *Science* 1971, *170*, 440–451.
[68] Rodbard, D., Chrambach, A., *Anal. Biochem.* 1971, *40*, 95–134.
[69] Slater, G. W., Rousseau, J., Noolandi, J., Turmel, C., Lalande, M., *Biopolymers* 1988, *27*, 509–524.
[70] Viovy, J. L., Duke, T., Caron, F., *Contemporary Physics* 1992, *33*, 25–40.
[71] Orbán, L., Chrambach, A., *Electrophoresis* 1991, *12*, 241–246.
[72] Tietz, D., Chrambach, A., *Anal. Biochem.* 1987, *161*, 395–411.
[73] Tietz, D., Chrambach, A., *Electrophoresis* 1992, *13*, 286–294.
[74] Tietz, D., Chrambach, A., *Electrophoresis* 1993, *14*, 185–190.
[75] Lumpkin, O. J., Zimm, B. H., *Biopolymers* 1982, *21*, 2315–2316.
[76] Lumpkin, O. J., Déjardin, P., Zimm, B. H., *Biopolymers* 1985, *24*, 1573–1593.
[77] Klotz, L. C., Zimm, B. H., *J. Mol. Biol.* 1972, *72*, 779–800.
[78] Southern, E. M., *Anal. Biochem.* 1980, *105*, 304–318.
[79] Slater, G. W., Noolandi, J., *Biopolymers* 1989, *28*, 1781–1791.
[80] Bode, H.-J., *Z. Naturforschung* 1979, *34c*, 512–528.
[81] Bode, H. J., in: Radola B. J., (Ed.), *Electrophoresis '79,* W. de Gruyter, Berlin 1980, pp. 39–52.
[82] Griess, G. A., Moreno, E. T., Easom, R. A., Serwer, P., *Biopolymers* 1989, *28*, 1475–1484.
[83] Jones, H. K., Ballou, N. E., *Anal. Chem.* 1990, *62*, 2484–2490.
[84] Boček, P., Chrambach, A., *Electrophoresis* 1991, *12*, 620–623.
[85] Burroughs, J. A., Chrambach, A., *Biochem. Biophys. Res. Comm.* 1991, *180*, 1070–1074.
[86] Guszcynski, T., Garner, M. M., Deml, M., Chrambach, A., *Appl. Theor. Electrophoresis* 1991, *2*, 151–157.
[87] Grossman, P. D., Colburn, J. C., Lauer, H. H., *Anal. Biochem.* 1989, *179*, 28–33.
[88] Grossman, P. D., Colburn, J., *Capillary Electrophoresis: Theory and Practice.* Academic Press, San Diego 1992, Chapter 4.
[89] Hjertén, S., *J. Chromatogr.* 1985, *347*, 191–198.
[90] Hjertén, S., Kubo, K., *Electrophoresis* 1993, *14*, 390–395.
[91] Petorius, V., Hopkins, B. J., Schieke, J. D., *J. Chromatogr.* 1974, *99*, 23–30.
[92] McIntire, G. L., *J. Microcolumn Sep.* 1990, *2*, 176–179.
[93] Belder, D., Schomburg, G., *J. High Res. Chromatogr.* 1992, *15*, 686–693.
[94] Smith, J. T., El Rassi, Z., *Electrophoresis* 1993, *14*, 396–406.
[95] Lehninger, A. L., Nelson, D. A., Cox, M. M., *Principles of Biochemistry* Worth Publishers, New York 1993, p. 330.
[96] Bae, Y. C., Soane, D. S., *J. Chromatogr.* 1993, *652*, 17–22.
[97] Rodbard, D., in: Catsimpoolas, N., (Ed.), *Methods of Protein Separation,* Plenum Press, New York 1976, p. 145.
[98] Tietz, D., Aldroubi, A., Pulyaeva, H., Guszczynski, T., Garner, M. M., Chrambach, A., *Electrophoresis* 1992, *13*, 614–616.
[99] Guszczynski, T., Chrambach, A., *Biochem. Biophys. Res. Comm.* 1991, *179*, 482–486.
[100] Boček, P., Chrambach, A., *Electrophoresis* 1991, *12*, 1059–1061.
[101] Garner, M. M., Chrambach, A., *Electrophoresis* 1992, *13*, 176–178.
[102] Tietz, D., Chrambach, A., *Electrophoresis* 1986, *8*, 241–250.
[103] Tietz, D., Gombocz, E., Chrambach, A., *Electrophoresis* 1987, *8*, 271–286.
[104] Brown, W., *Arkiv for Kemi* 1961, *18*, 227–285.
[105] Cantor, C. R., Schimmel, P. R., *Biophysical Chemistry, Part III: The Behavior of Biological Macromolecules.* W. H. Freeman, New York 1980.
[106] Ferry, J. D., *Viscoelastic Properties of Polymers* John Wiley, New York 1961, Chapter 10.
[107] Bueche, F., *Physical Properties of Polymers* John Wiley, New York 1962.